Casa abierta al tiempo
UNIVERSIDAD AUTÓNOMA METROPOLITANA
Unidad Iztapalapa

DIVISIÓN DE CIENCIAS BIOLÓGICAS Y DE LA SALUD
POSGRADO EN BIOLOGÍA EXPERIMENTAL

"CARACTERIZACIÓN DE LOS EFECTOS DE LA PROTEÍNA MCL-1 INDUCIDA POR EL COLESTEROL EN CÉLULAS DERIVADAS DE UN HEPATOCARCINOMA HUMANO"

T E S I S

Para obtener el grado de

Maestro en Biología Experimental

PRESENTA

Lic. En Biol. Exp Jonathan González Ruíz

Comité Tutoral

Director: Dr. Luis Enrique Gómez Quiroz

Director: Dr. Cédric Coulouarn

Asesora: Dra. Roxana U. Miranda Labra

Casa abierta al tiempo
UNIVERSIDAD AUTÓNOMA METROPOLITANA
Unidad Iztapalapa

DIVISIÓN DE CIENCIAS BIOLÓGICAS Y DE LA SALUD
POSGRADO EN BIOLOGÍA EXPERIMENTAL

"CHARACTERIZATION OF MCL-1 EFFECTS INDUCED BY CHOLESTEROL IN CELLS DERIVED FROM HUMAN HEPATOCARCINOMA"

T H E S I S

To obtain Master´s degree

in Experimental Biology

Author

Bachelor´s of Exp. B Jonathan González Ruíz

Commitee

Director: Luis Enrique Gómez Quiroz PhD.

Director: Cédric Coulouarn PhD.

Advisor: Roxana U. Miranda Labra PhD

El Programa de Doctorado en Biología Experimental de la Universidad Autónoma Metropolitana pertenece al Programa Nacional de Posgrados de Calidad (PNPC) del CONACYT, registro 001482, en el Nivel Consolidado, y cuenta con apoyo del mismo Consejo, clave DAFCYT-2003IDPTNNN0020.

Este trabajo fue realizado en el laboratorio de Fisiología Celular, del Departamento de Ciencias de la Salud de la Universidad Autónoma Metropolitana, Unidad Iztapalapa/ Laboratorio de Medicina Experimental, Unidad de Medicina Translacional, Instituto de Investigaciones Biomédicas, UNAM/Instituto Nacional de Cardiología Ignacio Chávez, México bajo la dirección del doctor Luis E. Gómez Quiroz y en el Institut national de la santé et de la recherche médicale (Inserm), Laboratorio de Liver Metabolisms and Cancer, (NUMECAN), University of Rennes, Francia, bajo la dirección del doctor Cedric Coulouarn.

El trabajo de investigación fue patrocinado por el Consejo Nacional de Ciencia y Tecnología (CONACYT) Fronteras de la Ciencia 1320, bajo la responsabilidad técnica del Dr. Luis E Gómez-Quiroz, INFR-2017-280788 bajo la responsabilidad técnica de la Dra. Ma. Concepción Gutiérrez Ruiz.

Durante el transcurso de la Maestría en Biología Experimental, en la UAM-Iztapalapa, recibí la beca otorgada por el CONACYT, con número de becario/CVU 615971/793513, en el período 2016-2018, así mismo conté con la beca mixta o de movilidad que me permitió realizar una estancia en la Universidad de Rennes, Francia, en el Laboratorio del Dr. Cédric Coulouarn. Agradezco al CONACYT su apoyo

Los miembros del jurado, designados por la Comisión Académica del Posgrado en Biología Experimental de la División de Ciencias Biológicas y de la Salud de la universidad Autónoma Metropolitana-Iztapalapa, abajo firmantes, aprobaron la tesis **"CARACTERIZACIÓN DE LOS EFECTOS DE LA PROTEÍNA MCL-1 INDUCIDA POR EL COLESTEROL EN CÉLULAS DERIVADAS DE UN HEPATOCARCINOMA HUMANO"** que presenta Jonathan González Ruíz con fecha del examen 6 de septiembre de 2018.

MIEMBROS DEL JURADO

PRESIDENTE
Dr. Javier Jimenez Salazar
Profesor titular B.
Departamento de Biología de la Reproducción
Universidad Autónoma Metropolitana

SECRETARIA
Dra. Mayra Domínguez Pérez
Laboratorio de Genómica de Enfermedades Cardiovasculares
Instituto Nacional de Medicina Genómica

VOCAL
Dra. Roxana U. Miranda Labra
Departamento de Ciencias de la Salud
Universidad Autónoma Metropolitana

VOCAL
Dr. Benjamín Pérez Aguilar
Departamento de Ciencias de la Salud
Universidad Autónoma Metropolitana

COMITÉ TUTORAL

DIRECTOR

Dr. Luis Enrique Gómez Quiroz

Laboratorio de Fisiología Celular, Departamento de Ciencias de la Salud, Universidad Autónoma Metropolitana unidad Iztapalapa, Edificio S, Laboratorio 351/Laboratorio de Medicina Experimental, Unidad de Medicina Translacional, Instituto de Investigaciones Biomédicas, UNAM/Instituto Nacional de Cardiología Ignacio Chávez, México.
legq@xanum.uam.mx

DIRECTOR

Dr. Cédric Coulouarn

Inserm, UMR 991, Liver Metabolisms and Cancer, University of Rennes 1, 35033 Rennes, France, CHU Pontchaillou,
2 rue Henri Le Guilloux, F-35033 Rennes, France.
cedric.coulouarn@inserm.fr

ASESORA

Dra. Roxana U. Miranda Labra

Laboratorio de Fisiología Celular, Departamento de Ciencias de la Salud, Universidad Autónoma Metropolitana unidad Iztapalapa, Edificio S, Laboratorio 351/Laboratorio de Medicina Experimental, Unidad de Medicina Translacional, Instituto de Investigaciones Biomédicas, UNAM/Instituto Nacional de Cardiología Ignacio Chávez, México.
rox_miranda20@hotmail.com

Agradecimientos

Al ***Dr. Luis Enrique Gomes Quiroz*** por su excepcional forma de coordinar este proyecto, por ser un gran ejemplo e inspiración, sin duda el mejor maestro que cualquier alumno podría tener, por su apoyo y sabiduría muchas gracias.

To ***Dr. Cédric Coulouarn*** thank you so much for supporting me, giving me the opportunity to use his skills and scientific expertise in this project. To show me the greatness of his county, to be my friend and also to be easier my academic stay.

A la ***Dra. Concepción Gutiérrez Ruiz*** quien se encuentra al frente del laboratorio con singular encanto; por buscar siempre nuevas oportunidades para todos los que formamos parte de este gran equipo, por su apoyo muchas gracias.

Dra. Roxana U. Miranda Labra por su apoyo y orientación en todo este proyecto muchas gracias.

A todo el equipo que conforma el **Laboratorio de Fisiología Celular/Medicina Experimental**. (Sha, Edwin, Isme, Monse, Soraya, Arturo, Ale, Jos, Gibran) y a los doctores Lety, Vero y Benja muchas gracias.

A **mis Amigos** quienes son parte importante en todo esto. (Manolo, Jeo, Kanka, Paco,) (Moy, Dante, Maly) todos ustedes son sumamente especiales en esta travesía.

Dedicatoria

A *mi* ***Madre*** por ser el pilar fundamental en todo lo que soy, en toda mi educación, tanto académica, como de la vida, por su incondicional apoyo perfectamente mantenido a través del tiempo.

“Todo este trabajo ha sido posible gracias a ti”

A ***Sharik*** quien es la única certeza que conservo en esta locura que he convenido en llamar vida, por decidir vivir el camino de la ciencia a mi lado, por luchar cada batalla como uno mismo, por ser mi fuente de inspiración día a día. Gracias.

“Toda nuestra ciencia, comparada con la realidad, es primitiva e infantil... y sin embargo es lo más preciado que tenemos.”

Albert Einstein

Introducción.

El carcinoma hepatocelular.

El carcinoma hepatocelular (HCC) es el tumor primario más frecuente en el hígado y su incidencia nivel global del cáncer primario en hígado ha incrementado progresivamente durante las últimas décadas (He et al., 2017). Entre las neoplasias malignas del hígado, el carcinoma hepatocelular es el más prevalente y afecta a cerca de un millón de individuos anualmente a nivel mundial, con una incidencia anual de 500 mil a 1 000 mil de casos al año, la tasa de mortalidad es aproximadamente igual a su incidencia (Cronin et al., 2018)mientras, que a nivel nacional las enfermedades crónicas del hígado ocupan el cuarto lugar de las principales causas de mortalidad. Por otra parte, en la población en edad productiva (15-64 años) ocupan el segundo lugar, siendo evidente la importancia de las enfermedades hepáticas como un problema de salud pública.

Enfermedad de hígado graso no alcohólico

La esteatosis no alcohólica o hígado graso no alcohólico (NAFLD), por sus siglas en inglés, Non-alcoholic Fatty Liver Disease fue descrita por Ludwing et al., (1980) como un patrón morfológico de lesión hepática en pacientes principalmente con obesidad y diabetes mellitus, en los cuales no existen antecedentes de consumo y/o abuso de alcohol, que histológicamente muestran cambios similares a los que se observan en la esteatohepatitis alcohólica (ASH) (Liu, Baker, Bhatia, Zhu, & Baker, 2016).

El papel del colesterol en la esteatohepatitis ha captado cada vez más atención en los últimos años y actualmente se considera un factor clave en ASH y esteatohepatitis no alcohólica (NASH). Aunque la patogénesis de estas enfermedades es diferente

presentan características histológicas indistinguibles y mecanismos subyacentes comunes.

El colesterol es constituyente esencial en las membranas biológicas, el cual juega un papel clave en las propiedades fisiológicas y en la regulación de vías de señalización. Debido a la regulación que ejerce en la fluidez de las membranas. El colesterol es un determinante importante en la permeabilidad relativa de la bicapa lipídica y se encuentra distribuido de manera heterogénea entre las membranas, (Ribas, Garcia-Ruiz, & Fernandez-Checa, 2016). El colesterol induce el empaquetamiento de la membrana en microdominios específicos de la membrana plasmática, proporcionando una plataforma para una variedad de proteínas de señalización asociadas a la membrana (Ribas, Garcia-Ruiz, & Fernandez-Checa, 2014). No todas las bicapas celulares presentan en su composición los mismos niveles de colesterol, éste es particularmente abundantemente en la membrana plasmática (Ikonen, 2008).

El colesterol y enfermedad hepática

El colesterol no esterificado se localiza principalmente en la membrana plasmática donde se forman dominios específicos. El transporte de colesterol mitocondrial es realizado preferentemente por Stard1, que regula el transporte de colesterol desde la membrana externa hasta la membrana interna mitocondrial de esta forma contribuyen en la regulación de los niveles de colesterol en la membrana para evitar su acumulación. (Enriquez-Cortina et al., 2013)

La acumulación de colesterol en las mitocondrias disminuye la fluidez de las membranas mitocondriales, lo cual aumenta el umbral de permeabilización de la membrana externa mitocondrial mediante la reestructuración de las bicapas de la membrana mitocondrial (Ribas et al., 2016), la acumulación de colesterol mitocondrial puede contribuir indirectamente a los cambios metabólicos de las células cancerosas por el deterioro de la función mitocondrial y la activación de los programas de supervivencia (Maierean et al., 2017).

Las células cancerosas exhiben cambios metabólicos críticos inducidos por mutaciones, que provocan un incremento en la función de oncogenes y la pérdida de la función de genes supresores de tumores. Esto resulta en la alteración en el metabolismo celular, desregulación del crecimiento, resistencia a la muerte celular, invasión y metástasis (Hanahan & Weinberg, 2011). Muchas de estas características son reguladas por cambios en la función mitocondrial y, tal vez, por modificaciones en el metabolismo del colesterol, así como en su transporte hacia la mitocondria.

La mitocondria

La mitocondria es una de las principales fuentes de especies reactivas de oxígeno (ERO) (Venditti et al, 2013), por lo que se requiere de un sistema antioxidante eficaz. El glutatión mitocondrial (mGSH) es un componente central, previene o repara el daño oxidante generado durante el metabolismo aeróbico normal (Ribas et al., 2014). La generación primaria de las ERO en las mitocondrias es el anión superóxido, el cual es producido en la matriz mitocondrial, este puede ser dismutado hacia peróxido de hidrógeno (H_2O_2) esta reacción es catalizada por la su peróxido dismutasa (SOD2) (Mari et al., 2010). Las series de eventos que llevan a la apoptosis se han categorizado

en dos modos, las vías apoptóticas extrínsecas e intrínsecas (Li & Dewson, 2015). Las proteínas anti-apoptóticas de la familia de Bcl-2 están formadas por varios dominios homólogos (BH1 a BH4), especialmente el dominio BH3 les permite unirse a otras proteínas de la misma familia. Entre las proteínas más importantes de esta familia son por sus siglas en ingles B-cell lymphoma 2 y B-cell lymphoma-extra large (Bcl-2 Bcl-XL) y leucemia celular mieloide 1 (Mcl-1), su localización es generalmente mitocondrial pero también se han encontrado en retículo endoplásmico y en la membrana nuclear (Li & Dewson, 2015).

Mcl-1

Es un miembro pro-sobrevivencia de la familia Bcl-2 cuyo gen se identificó inicialmente como un gen de expresión temprano durante la diferenciación de células de leucemia mieloides (Elgendy et al., 2017). Algoritmos de alineación identificaron similitud en la secuencia proteica de supervivencia de Bcl-2, por ello cuando se descubrió Mcl-1 constituyó el segundo miembro de esta familia de proteínas (Elgendy & Minucci, 2015). La familia Bcl-2 se ha considerado una nueva clase de genes que promueven la oncogénesis, aunque no lo hace a través de la regulación positiva de la proliferación, sino manteniendo la viabilidad a través de la inhibición de la apoptosis (Schwickart et al., 2010). La desregulación de la expresión y la función de la familia de proteínas Bcl-2 se ha implicado desde entonces en todas las neoplasias (Zhen et al., 2017).

El incremento en la expresión de Mcl-1 puede contribuir al cáncer, de hecho, alteraciones en la expresión de Mcl-1 como ocurre en otras proteínas de esta familia, sirven como indicadores de respuesta a la enfermedad en pacientes con cáncer: por ejemplo, una expresión elevada de *mcl-1* está asociada con una progresión acelerada

de la enfermedad, así como una disminución en la respuesta a la terapia Mcl-1 bloquea la progresión de la apoptosis por unión y secuestro de las proteínas pro-apoptóticas por sus siglas en inglés Bcl-2-like protein 11 y BCL2 Associated X (Bim y Bax), que son capaces de formar poros en la membrana mitocondrial permitiendo la liberación de citocromo c en el citoplasma e induciendo la activación de caspasas responsables de gran parte de la degradación macromolecular observada durante la apoptosis (Thomas et al., 2010).

Justificación

La evolución de NAFLD a HCC es un proceso lento, que puede tomar hasta 30 años, por lo que datos concretos de la relación hígado graso HCC no existen por el momento. En la actualidad, el aumento en el consumo de alimentos con alto contenido calórico está originando un incremento en la obesidad y en el síndrome metabólico. Se sabe que México ocupa el segundo lugar en obesidad en adultos a nivel mundial y el primero en obesidad infantil (Aceves-Martins, Llaurado, Tarro, Sola, & Giralt, 2016). Dados los datos anteriores es fácilmente predecible que en los próximos 20 años se observará un aumento alarmante en casos de HCC, siendo más preocupante el hecho de que puede presentarse en edades tempranas. Recientemente el Instituto Nacional de Cáncer de los Estados Unidos (NCI/NIH), reportó en su “Annual report to the nation on the status of cancer, 1975-2012” (Ryerson et al., 2016), que la mortalidad general por cáncer está disminuyendo significativamente, sin embargo, cuatro neoplasias se incrementan lejos de disminuir, siendo el de hígado el que mayor incremento tiene (lo cual representa en sí mismo ya una alerta internacional).

Datos de nuestro laboratorio (Enriquez-Cortina et al., 2017), muestran que, tanto la sobrecarga de colesterol y de lípidos están asociados con un mal pronóstico en HCC; de hecho, la sobrexpresión génica de proteínas relacionadas con lipogénesis muestra un fenotipo más agresivo en HCC. El incremento en marcadores de tumorogenicidad, como lo es la proliferación, se encuentran regulados al alza, lo que indica una desregulación en proteínas anti-apoptóticas como lo es Mcl-1. Por lo que entender el papel que desempeña Mcl-1 en el HCC es de suma importancia.

Pregunta de investigación

¿Cuál es el papel que tiene Mcl-1 en el carcinoma hepatocelular con sobrecarga de colesterol?

Hipótesis

La sobrecarga de colesterol en células de HCC incrementa el fenotipo agresivo en un mecanismo dirigido por la sobreexpresión de Mcl-1

Objetivo general

Determinar la relación entre la sobrecarga de colesterol y la expresión de Mcl-1 con parámetros de tumorigenicidad celular.

Objetivos particulares

1.- Determinar la relación de la sobrecarga de colesterol con la expresión de Mcl-1 en células tumorales.

2.- Caracterizar el mecanismo por el cual la sobrecarga de colesterol induce la sobreexpresión de Mcl-1.

3.-Determinar el papel Mcl-1 en los parámetros de malignidad celular en un ambiente con sobrecarga de colesterol.

4.- Caracterizar los parámetros tumorigénicos en líneas celulares derivadas de hepatocarcinomas con el gen Mcl-1 silenciado y sobreexpresado en un ambiente con sobrecarga de colesterol.

Diseño Experimental

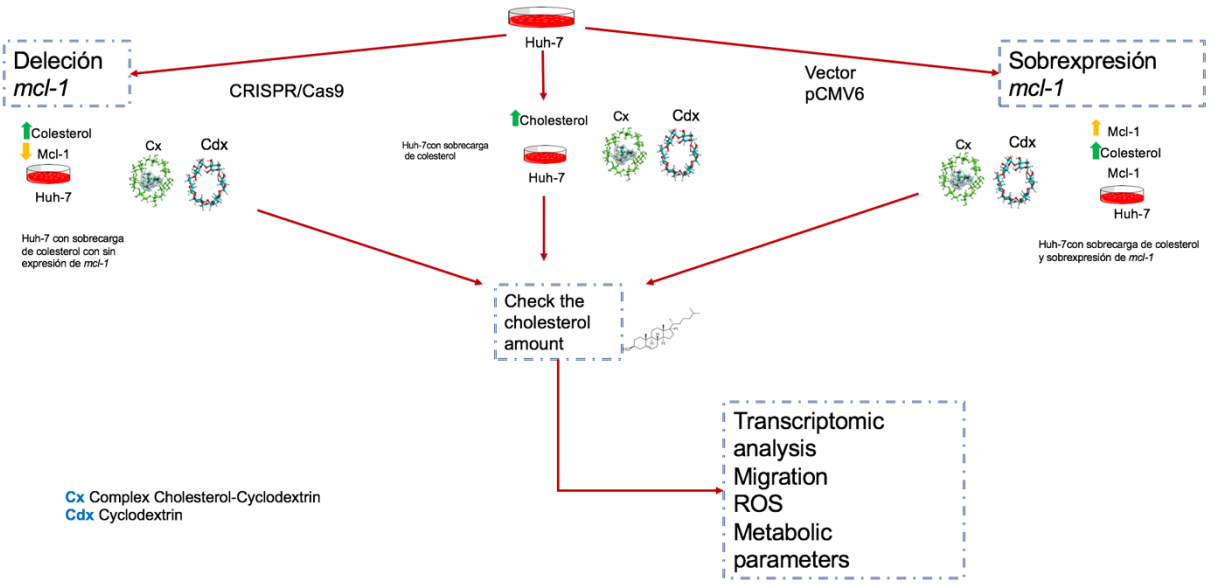

Metodología

Cultivo celular: Se obtuvo una línea Huh7 de células HCC humanas de ATCC.

Las líneas celulares se sembraron a 48 000 células/cm2 en placas de Petri (Corning, EE. UU.) Utilizando medio Williams E para Huh7, suplementado con suero bovino fetal al 10% (v/v) (FBS, Hyclone Laboratories Inc., Logan Utah, EE. UU.) Las células se incubaron a 37°C (5% de CO_2 y 95% de aire a humedad de saturación) y se verificó la adherencia de la monocapa después de 4 h. Una vez adheridas, las células se lavaron con solución salina fosfatos (PBS) y el medio se reemplazó por un medio de crecimiento sin suero, las células se trataron con el complejo colesterol-ciclodextrina (Cx) y ciclodextrina (Cdx) durante 90 min. El colesterol y Ciclodextrina se adquirieron de Sigma.

Western blot: el análisis de transferencia Western se realizó como se describe en estudios previos de nuestro grupo (Enriquez-Cortina et al., 2017). Las células se lisaron con M-PER reactivo de extracción de proteína de mamífero (Thermo Scientific) complementado con inhibidor de proteasas e inhibidor de fosfatasas COMPLETE y phosSTOP respectivamente (Roche Diagnostics, Barcelona, España), se centrifugó a 12.879 g durante 15 min a 4°C. Los sobrenadantes se colectaron y las concentraciones de proteína se determinaron con kit de ensayo de ácido bicinconínico (kit de ensayo de proteínas PierceTM BCA, Thermo Scientific). La proteína (80-100µg/ml) se usó en SDS-PAGE al 10% y se transfirió a membranas de PVDF de 0,2 m de baja fluorescencia (GE Healthcare Life Sciences). Después de bloquear con leche sin grasa

al 5% a 4°C durante 1 h, las membranas se probaron con anticuerpos contra las proteínas de interés (dilución 1:1000) y β-actina como gen de normalización (dilución 1:10.000) a 4ºC durante toda la noche. Después de tres lavados con TBS, la membrana se incubó con anticuerpo secundario acoplado a peroxidasa de rábano a temperatura ambiente durante 2 h y se usó según los anticuerpos primarios. Las membranas se revelaron usando Luminol®. Las bandas de proteínas se escanearon y las intensidades de la banda se cuantificaron usando un densitómetro Imaging System (Gel Logic 1500, Kodak).

Ensayos de cierre de heridas. Según lo informado por (Jiménez-Salazar et al., 2014), las células Huh-7 se cultivaron al 100% de confluencia. Las células se mantuvieron en medio de cultivo durante 24 h antes de generar la "herida" (rasgado), y luego los tratamientos (Cx 160μg/ml, Cdx10mM) se complementaron a los pocillos durante 4, 12, 24 o 48 h. Las heridas lineales (aproximadamente 0,7 mm de ancho) se hicieron suavemente con una punta de pipeta estéril a través de la superficie de cultivo; las placas se lavaron con PBS para eliminar los restos. Para mostrar que el cierre de heridas se debe a la migración celular en lugar de la proliferación celular inducida por Cx, las células también se incubaron en ausencia y presencia de hidrocloruro de citosina β-d-arabinofuranosida 10 μM, un inhibidor de la síntesis de ADN, a las 48 h de Cx.

Determinación del colesterol libre con tinción y cuantificación con filipina: las células se fijaron con PFA al 4% durante 15 min a temperatura ambiente. Para la determinación de colesterol libre, las células se incubaron con filipina como se informó previamente (Rosales-Cruz et al., 2018).

Determinación del colesterol: $2x10^6$ células en 100 µL de PBS se saponificaron con KOH alcohólico en un bloque de calentamiento a 60ºC durante 15 min. Después de que la mezcla se había enfriado, se añadieron 2 ml de hexano y 600 ml de agua destilada y se agitaron para asegurar la mezcla completa. Las alícuotas apropiadas de la capa de hexano se evaporaron usando el concentrador SpeedVac y se usaron para la medición del colesterol con reactivo de O-ftalaldehído (OPA) (Sigma-Aldrich) disuelto en ácido acético; después se añadió ácido sulfúrico y luego se leyó a 550 nm en el espectrofotómetro. como se reportó anteriormente (Domínguez-Pérez et al., 2016).

Determinación de ERO: Las células se trataron con Cx y Cdx durante 90 min, y las placas se incubaron de inmediato durante 15 min, en la oscuridad, a temperatura ambiente con 2 ', 7' - diclorofluoresce diacetato (DCFDA, 5 µM), como informamos previamente (Nuno-Lambarri et al., 2016).

Expresión de *mcl-1*: Reacción en cadena de la polimerasa de transcripción inversa cuantitativa (qRT-PCR), las reacciones se realizaron en el sistema de detección de

PCR en tiempo real Bio-Rad CFX96 Touch (Bio-Rad). se realizó como se describe (Coulouarn et al., 2012).

Perfiles de expresión génica: El perfil de expresión de todo el genoma se realizó utilizando el kit de etiquetado QuickAmp de baja aportación y microbandas pangenómicas SurePrint G3 8x60K de sondas humanas (Agilent Technologies, Santa Clara, CA) tal como se describe. (Coulouarn et al., 2012) los microarrays incluyen 26,083 genes y 30,606 lncRNAs. Los datos de expresión génica se procesaron utilizando Feature Extraction y el software GeneSpring (Agilent Technologies).

Edición genética por CRISPR/Cas9: El plásmido PX458. se obtuvo de Addgene (# 48138, 32), tiene un gen de resistencia a la ampicilina para la selección en bacterias, también contiene la secuencia del gen hSpCas9 de S. pyogenes unida al gen GFP por la secuencia del péptido 2A para la coproducción de ambas proteínas, la expresión de ambos genes está dirigida por un promotor de CAG sintético. Además, el plásmido contiene las secuencias necesarias para la expresión de los ARN guía.

La respiración mitocondrial en tiempo real (OCR) y la tasa glucolítica (ECAR): se controlaron con el Seahorse XF24 Flux Analyzer (Seahorse Bioscience) de acuerdo con las instrucciones del fabricante. Para la evaluación del ECAR en tiempo real, las células se incubaron con medio de ensayo no tamponado (XF Media Base que contiene L-glutamina 2 mM) seguido de una inyección secuencial de glucosa 10 mM, oligomicina 2 µM y 2-desoxiglucosa 50 mM. Para las células OCR se incubaron con

medio de ensayo no tamponado (XF Media Base con glucosa 25 mM, L-glutamina 4 mM y piruvato 5 mM) seguido de una inyección secuencial de oligomicina 2 µM, cianuro de carbonilo 0,2 µM 4- (trifluorometoxi) fenilhidrazona y 2 µM antimicina A más Rotenona. Ambas mediciones de ECAR y OCR se normalizaron a g de proteína total después del ensayo de proteína Bradford. como se informó anteriormente (Baulies et al., 2018)

Análisis estadístico: los datos se presentan como media ± S.E. para al menos tres experimentos independientes llevados a cabo por triplicado. Las comparaciones entre los grupos se realizaron usando la prueba ANOVA con un análisis post hoc de Tukey. Las diferencias se consideraron significativas a $p < 0.05$. El software Prism versión 6 se utilizó para ejecutar el análisis.

Resultados

Validación de la estabilidad y localización de la incorporación de colesterol

Se validó el modelo in vitro de incorporación de colesterol en células derivadas de cáncer de hígado. La Figura 1a muestra el aumento en el contenido de colesterol en las células Huh-7 tratadas con el Cx durante 90 min, este aumento representa 10 veces más contenido de colesterol que las células no tratadas, por otro lado, las células tratadas con Cdx muestran disminución en la cantidad de colesterol en comparación con las no tratadas, es importante mencionar que el impacto de la sobrecarga de colesterol in vitro, debe representar los valores fisiológicos reportados (Rosales-Cruz et al., 2018). Usamos la línea celular HepG2 solo para validar, que la incorporación del

colesterol no fue exclusivamente para la línea celular Huh-7 (Figura 1b). También se llevaron a cabo experimentos en hepatocitos primarios de ratón alimentados con una dieta de chow, para corroborar que el modelo no solo funcionaba en células transformadas, sino que también se podía usar en células sin algún tipo de mutación, por lo que las células se trataron con 160μg/mL de Cho y Cdx durante 90 min, respectivamente, y se observó un incremento de 6 veces en comparación con el control (Figura 1c).

Para determinar una concentración que representa un efecto similar a los ratones alimentados con una dieta alta en colesterol, se usaron diferentes concentraciones, y la concentración que tuvo efectos similares *in vivo* es de 160μg/mL ya que esta aumentó alrededor de 4 a 5 veces la cantidad de colesterol, respecto al control, (Figura 1d)

Para determinar si el colesterol que se incorporó a la línea celular permaneció dentro de la célula a lo largo de los experimentos, se cuantifico el colesterol hasta 72 h después de su incorporación, en el mismo experimento las células se trataron durante 72 h para determinar cuál era la mejor forma de incorporación. (Figura 1e)

La tinción con Filipina confirmó que el contenido de colesterol libre aumentó en las líneas celulares Huh-7 y Hep3B cuando son tratadas con Cx. Para abordar la localización del colesterol incorporado, las mitocondrias fueron marcadas con mitotracker, se puede observar que una parte importante del colesterol incorporado se

encontró en las mitocondrias, ahora realmente sabemos que nuestro modelo funciona, y es capaz de aumentar la cantidad de colesterol, en diferentes líneas celulares, en este momento usamos Hep3B. (Figura 2)

La sobrecarga de colesterol aumenta la migración celular.

Con el fin de evaluar los efectos fisiológicos de la sobrecarga de colesterol, se realizó una serie de ensayos de cierre de herida, tratamos células Huh-7 con Cx y Cdx. Observamos que las células con la mayor cantidad de colesterol tenían una mayor capacidad para cerrar la herida migrando más rápido en comparación con las células no tratadas (Figura 3). Para diferenciar que el proceso fue migración en lugar de proliferación, las células Huh-7 se incubaron en presencia de 10μM cytosine β-D arabinofuranoside hydrochloride 48h después de la adición de colesterol. Se observaron resultados similares en ausencia y presencia del inhibidor de la síntesis de ADN. (Jiménez-Salazar et al., 2014)

La sobrecarga de colesterol aumenta ERO.

Como se observó anteriormente en animales de experimentación (Gomez-Quiroz et al., 2016), la ingesta de colesterol a partir de la dieta induce la producción ERO. Para explorar si el mismo efecto se presenta en el modo *in vitro*, el contenido de ERO se midió mediante fluorescencia de DHE. Las células tratadas con colesterol aumentaron significativamente ERO. La Figura 4 muestra que el contenido de anión superóxido aumenta por la sobrecarga de colesterol a los 90 min de tratamiento, mientras que Cdx

no induce ningún cambio. Este incremento es consistente con los resultados de la motogénesis, debido a que las ERO se encuentran entre los principales inductores de la movilidad (Domínguez-Pérez et al., 2016).

La sobrecarga de colesterol induce la sobreexpresión de Mcl-1.

Dado que la sobrecarga de colesterol desempeña un papel muy importante en la inducción del cáncer (Yu, Liu, Chen y Lin, 2016), decidimos observar si la sobrecarga de colesterol induce la expresión de Mcl-1, así como algunas proteínas de la familia de Bcl2, como BclXL. Se encontró que la sobrecarga de colesterol indujo un aumento en el contenido de proteína de la isoforma anti-apoptótica de Mcl-1, sin embargo, no se encontraron efectos en los otros miembros de la familia, tales como BclXL y Bcl2, así mismo medimos el contenido proteico de Stat3 quien es el factor de transcripción de Mcl-1, y observamos que el Cx induce la expresión de Stat3 (Figura 5a). Corroboramos el resultado *mcl-1* por qRT-PCR, (Figura 5b). La relevancia en la expresión de *mcl-1*, particularmente en las células cancerosas, sugiere fuertemente una posible promoción del tumor característica del colesterol. Para verificar esto, alimentamos a ratones con una dieta alta en colesterol (1% de colesterol) durante 3 meses y recibieron una dosis única de diethylnitrosamine (DEN) (10μg/g) como carcinógeno, y el contenido de proteína de Mcl-1 se determinó en tumores (T) y tejido circundante (ST), la figura 7 muestra que ciertamente la ingesta de colesterol aumenta la expresión de esta proteína antiapoptótica en tejido maligno y premaligno. (Figura5c).

Supresión de mcl-1.

Para analizar de manera más profunda la relevancia de Mcl-1 inducido por colesterol, se desarrolló un sistema CRISPR / Cas9, para evaluar el papel de Mcl-1 en el contexto de sobrecarga de colesterol, nuestros resultados muestran que Mcl-1 es una proteína importante para el desarrollo de cáncer, hay varios informes donde postulan a Mcl-1 como posible blanco terapéutico, dada la naturaleza de esta proteína, está involucrada en la proliferación celular (Harley, Allan, Sanderson y Clarke, 2010), el metabolismo energético y la dinámica mitocondrial (Perciavalle et al., 2012). Mcl-1 es uno de los genes más altamente amplificados en una variedad de HCC (Sieghart et al., 2006). Como resultado, la mayoría de las estrategias terapéuticas se han dirigido a antagonizar la actividad antiapoptótica Mcl-1 que intenta fomentar la muerte celular maligna (Yu et al., 2016).

Entonces se realizó un Knockout para evaluar la función Mcl-1 cuando esta proteína se activa para la sobrecarga de colesterol.

Diseño de ARNs guías.

Para diseñar los ARNs guías (ARNg) se tomaron secuencias de ARN del gen *mcl-1* (exón 1 5,831-6,045 y exón 2 8,379-8,469). (tabla 1) Una vez que se obtuvieron las secuencias, se utilizó el software Broad Institute (disponible en http://www.broadinstitute.org/rnai/public/analysis-tools/sgrna-design), que proporcionó las mejores secuencias candidatas de ARNg para los objetivos planificados (Figura 6a).

Para determinar el knockout de *mcl*-1, se realizó un Western Blot contra Mcl-1, donde podemos observar que el contenido de proteína es significativamente menor en comparación con su control. Esto significa que se realizó exitosamente el knockout de *mcl-1* con CRSPER / cas9. Usamos Hek-293 porque es una línea celular permisiva para transfectar, observamos que fue necesario la combinación de los tres ARNg para obtener el knockout en ambas líneas celulares. (Figura 6b).

Una vez que se corroboró la supresión de *mcl-1*, decidimos usar algunas combinaciones de ARNg para encontrar solo una deleción específica de *mcl*-1L, para realizar esta deleción específica usamos ARNg 1 y ARNg 2 (Figura 10), por lo que con esta deleción específica se puede saber si la sobrecarga de colesterol induce solo la isoforma larga de *mcl*-1 o la sobrecarga de colesterol puede inducir todas las isoformas de Mcl-1. Varios estudios muestran que la isoforma larga es uno de los factores implicados y la sobreexpresión en el cáncer (Gruber et al., 2013; V. Palve, Mallick, Ghaisas, Kannan y Teni, 2014; V. C. Palve & Teni, 2012).

Para determinar el papel de Mcl-1L en la agresividad celular, se realizó una prueba de cierre de heridas en células Huh-7 Δ*mcl-1L*. Los datos sugieren que Mcl-1L participa en la motilidad celular, ya que en la línea celular Δ*mcl-1L* las células migraron más lentamente que Huh-7, a las 72h, Huh-7 cerró completamente la herida, pero no la línea celular Δ*mcl-1L*, incluso cuando se agregó Cx, el cierre de la herida no se completó (Figura 15), la sobrecarga de colesterol induce la migración celular incluso

sin la presencia de Mcl-1L, con Cdx se observó que tanto en la migración de las células ∆*mcl-1L* como Huh-7 se vio afectada.

El papel de Mcl-1 como un modulador metabólico en células de hepatocarcinoma.

Debido a que Mcl-1L podría estar relacionado con la regulación del metabolismo celular (Thomas et al., 2010), se decidió explorar cualquier cambio en el metabolismo bioenergético. Al utilizar la tecnología Seahorse, se determinó el OCR, con el uso del kit de mitostres. Las células Huh-7 Mcl-1L tenían una mayor capacidad mitocondrial, es decir, la respiración máxima era mayor en Huh-7 *∆mcl-1L*, producción de ATP y respiración basal, lo que indica una clara relación entre Mcl-1L y el metabolismo. (Figura 12)

Los resultados sugieren que Mcl-1L podría ser un regulador metabólico, teniendo más puntos de comparación, está claro que el Mcl-1 es necesario para el metabolismo mitocondrial, dejando en claro que la isoforma antiapoptótica es la inducida por el colesterol, cuando comparamos todos los parámetros, como la producción de ATP, la fuga de protones, la línea celular Huh-7 a la que Mcl-1L tiene una mejor respuesta que Huh-7.

De la misma forma, la acidificación del medio extracelular se midió con el kit de Estrés Glicólitico de Seahorse, para determinar si la eliminación de la isoforma grande Mcl-1

solo induce el metabolismo mitocondrial. Lo que encontramos fue que la deleción de Mcl-1L también aumentó la acidificación del medio extracelular, por lo que la capacidad glucolítica, así como su reserva son mayores. Estos datos corroboran que Mcl-1L juega un papel importante en el metabolismo celular, de modo que la regulación de la actividad de esta proteína es un punto importante en la transformación celular. (Figura 13)

Análisis Transcriptómico global en línea celular Huh-7.

Es clara la gran relevancia del colesterol en la regulación de Mcl-1. Para explorar más a fondo, se decidió analizar los cambios transcriptómicos globales por Microarreglos. Decidimos realizar un método diferente para la regulación negativa de Mcl-1, con el fin de corroborar los resultados obtenidos con el Knockout de Mcl-1, de esta manera podemos asegurar que los datos obtenidos en la regulación metabólica por Mcl-1, sean propia de la proteína y no por mutación al azar relacionada con el sistema Cas9, por lo que realizamos un método menos agresivo donde solo podíamos disminuir la presencia de Mcl-1, por lo tanto, el uso de interferencia de ARN (ARNi), figura 17. Se realizaron diferentes diluciones (0,05 M, 0,1 M, 0,15 M) de siRNA-Mcl-1, estas diluciones no presentaron diferencias significativas, por lo que en los experimentos posteriores se utilizó 0,05M ARNi Mcl-1. (Figura 14).

Para comprender globalmente cómo la sobrecarga de colesterol afecta a la línea celular Huh-7, se llevó a cabo un estudio transcriptómico, en el que pudimos determinar los genes afectados por la sobrecarga de colesterol. El perfil transcriptómico entre las células con sobrecarga de colesterol y sin tratamiento fue 318

genes expresados diferencialmente. Estos genes están regulados al alza (RAB27B, ACSL3, BMF, ATP2B4, TPTE2P6, TPTE2, CYP2R, STARD9) y estos son algunos genes que están regulados negativamente (SREBF1, MVD, TP53INP1, HMGCR, CDKN1C, IGFBP1, CDKN1A). Encontramos que un número significativo de genes se regularon negativamente en relación con la biosíntesis del colesterol, lo cual es consistente con nuestro modelo de sobrecarga de colesterol. Curiosamente, también observamos que algunos genes relacionados con la inhibición del ciclo celular se regularon negativamente, por otro lado, en la lista de genes regulados a la alta se encontraron relacionados con el transporte de ácidos grasos. (Figura 17)

Discusión.

NAFLD es la causa más común de enfermedad hepática en todo el mundo, con una prevalencia del 15% -30% en poblaciones occidentales (Calzadilla y Adams, 2016), mientras que en la infancia la prevalencia estimada de NAFLD en niños obesos está aumentando a 40-70%. El sello distintivo de NAFLD es la acumulación de lípidos en los hepatocitos que define anomalías hepáticas que van desde la esteatosis simple hasta la esteatohepatitis no alcohólica con o sin desarrollo de cirrosis (Streba et al., 2015).

Datos anteriores en nuestro laboratorio demostraron que el consumo de una dieta rica en colesterol induce una sobrecarga de colesterol en el hígado y una respuesta compleja en los hepatocitos caracterizada por disfunción mitocondrial y estrés oxidativo (Enriquez-Cortina et al., 2017). Todos estos procesos podrían estar asociados con una gran agresividad celular hablando en términos de cáncer. Por esa

razón, desarrollamos una nueva forma de estudiar los efectos inducidos del colesterol en ratones, pero ahora in vitro mediante líneas celulares. Por lo tanto, utilizamos diferentes líneas celulares para incorporar una sobrecarga de colesterol y demostramos que nuestro modelo funciona en diferentes líneas celulares como Huh-7, HepG2, Hep3B y cultivo primario de hepatocitos de ratón, ahora, está claro que la incorporación de colesterol es completamente diferente en cada línea celular, esto podría asociarse con la capacidad de manejar el colesterol, las células Huh-7 aumentan entre 3 y 4 cuando las células se tratan con Cx 160 g / ml, pero las células HepG2 aumentan alrededor de 10 veces más que Huh-7, de la misma manera el cultivo de células primarias de 6 veces en comparación con el control. Es decir que todos los experimentos se realizaron con la misma concentración, pero las células incorporaron diferentes cantidades de colesterol, si queremos comparar todos los efectos de las líneas celulares de la sobrecarga de colesterol, primero es necesario determinar la concentración óptima de Cx, como en la célula Huh-7 línea.

Los diferentes organelos tienen un contenido de colesterol y composición lipídica distintos y estrechamente regulados, con una gran mayoría del 60-90% del colesterol total que reside en la membrana plasmática, el retículo endoplásmico y las mitocondrias tienen un contenido inferior (3-5% del colesterol celular total) y son muy sensibles a la pérdida de fluidez de la membrana inducida por el enriquecimiento del colesterol (Luo et al., 2017). En la figura 2 hay una imagen representativa de la línea celular Huh-7 y Hep3B para abordar el contenido de colesterol cuando las células se trataron con Cx, después de lo cual se marcó la mitocondria para saber si la sobrecarga

de colesterol podía penetrar en la mitocondrial. La sobrecarga de colesterol en el hígado se ha asociado fuertemente a una mejora del daño debido a un segundo insulto como alcohol, ligadura del conducto biliar o productos químicos, estos hallazgos han posicionado este lípido como un determinante clave en la progresión de la enfermedad hepática (Musso et al., 2013). Mari et al. (2006) informaron que la acumulación de colesterol libre, pero no los triglicéridos o los ácidos grasos libres, juegan un papel clave, porque se sensibiliza a la esteatohepatitis mediada por citocinas inflamatorias (EHNA). De acuerdo con estudios previos en nuestro laboratorio informaron que la sobrecarga de colesterol es un factor determinante que podría mantener o agravar el daño hepático inducido por el alcohol (Lopez-Islas et al., 2016).

De este modo realizamos un experimento de cierre de herida, esta vez para saber si la sobrecarga de colesterol aumenta la movilidad celular, basada en la figura 3, células Huh-7 de con la sobrecarga de colesterol tiene una mejor respuesta, por otro lado, cuando las células fueron solamente tratadas con Cdx (disminuye el colesterol), las células no responden al estímulo, la cdx es una familia de compuestos formados por moléculas de azúcar unidas en un anillo (oligosacáridos cíclicos). la industria alimentaria, Cdx se emplean para la preparación de productos libres de colesterol: la molécula de colesterol voluminosos e hidrófobo se aloja fácilmente dentro de los anillos de Cdx que se eliminan a continuación (de Oliveira et al, 2011; Marcolino, Zanin, Durrant, Benassi Mde. , Y Matioli, 2011).

ERO son las principales inductoras del daño del ADN y, en consecuencia, de las mutaciones. De hecho, particularmente las ERO derivadas de mitocondrias han sido implicadas en la iniciación, la progresión y la agresividad del cáncer (Ishikawa et al.,

2008). La Figura 5 muestra el incremento del anión superóxido cuando las células se trataron con Cx, pero no cuando las células se trataron con Cdx. Así encontramos de manera redundante que el colesterol induce un incremento en la cantidad de ERO como se había reportado previamente (Enríquez-Cortina et al., 2017).

Los datos en esta tesis muestran que no hay cambios en la proteína Bcl-2, cuando se trata con colesterol, sin embargo, Mcl-1 muestra un aumento en el contenido de la proteína (Figura 6), esto sugiere que el aumento de esta proteína permite la inhibición de la muerte celular. Considerando a Mcl-1 de gran relevancia, porque la eliminación de esta proteína antiapoptótica induce daño hepático, fibrosis y aumenta la susceptibilidad a la apoptosis en los hepatocitos (Vick et al., 2009).

Un alto contenido de Bax se asocia consistentemente con la disminución de la actividad de Bcl-2, una proteína pro-apoptótica, ya que el cociente entre el contenido de estas dos proteínas se calcula continuamente para estimar la tasa de supervivencia celular (Strasser, 2005). Sin embargo, el papel de otros miembros de la familia Bcl-2 como Mcl-1, que comparten la homología más alta con Bcl-2, se ha dejado de lado.

Es bien sabido que la expresión de Mcl-1 es inducida por la activación del factor de transcripción STAT3. Este factor de transcripción desarrolla una respuesta adaptativa a la agresión al hígado mediante la amplificación de genes que mantienen la homeostasis celular (Szczepanek et al., 2012). La Figura 6 muestra que la sobrecarga de colesterol induce la activación de STAT3 en Ser727. STAT3 es inactivo en el citosol, pero una vez activado por citoquinas o factores de crecimiento, se fosforila al nivel de Tyr 705. Canonicamente, esta activación en Ty705 desencadena la dimerización y la translocación al núcleo. Una vez que el núcleo del dímero de Stat3, es fosforilado por

MAPK en el residuo de Ser 727, de modo que puede unirse al ADN y dirigir la expresión de sus genes diana (Timofeeva et al., 2012, You et al., 2015)

También observamos que la sobrecarga de colesterol induce la expresión de STAT3, donde podemos observar su aumento máximo a los 90 min. Los datos sugieren que la sobrecarga de colesterol ejerce efectos sobre STAT3 para que proteínas blancas como Mcl-1 funcionen como proteínas protectoras, limitando así la apoptosis, es importante señalar que este efecto no se encontró en proteínas como Bcl-2 o incluso BclxL. Corroboramos la expresión de Mcl-1 inducida por la sobrecarga de colesterol en mRNA por q RT-PCR.

Para verificar esto, ratones fueron alimentados con una dieta alta en colesterol (1% de colesterol) durante 3 meses y recibieron una dosis única de DEN (10 μg /g) como carcinógeno, y el contenido de proteína de Mcl-1 se determinó en tumores (T) y tejido circundante (ST). encontramos que solo los ratones con HC tenían un incremento en la dieta de Mcl-1 en T y ST, pero no en los ratones, la dieta de Chow Mcl-1 no estaba presente en T y ST. por lo que estos datos corroboran que la sobrecarga de colesterol tiene un impacto en Mcl-1, este efecto se asocia con el aumento de STAT3.

Los estudios de deleción génica han demostrado que la expresión de Mcl-1 es crítica para la supervivencia de múltiples linajes celulares, a pesar de la expresión concomitante de otras proteínas BCL-2 pro-supervivencia (Opferman et al., 2005). Sin embargo, la razón fisiológica por la que Mcl-1 es esencial para promover la

supervivencia de tantos tipos de células diferentes (Perciavalle et al., 2012) sigue siendo difícil de alcanzar. En este estudio, revelamos un papel para Mcl-1 en la inducción de la sobrecarga de colesterol (Rinkenberger, Horning, Klocke, Roth y Korsmeyer, 2000).

Para entender la función de Mcl-1 en el contexto de la sobrecarga de colesterol se realizó un knockout de Mcl-1, creamos una nueva línea celular Huh-7 sin *mcl-1*, para deletar este gen se usó CRISPR / cas9, diseñamos tres ARNg (Tabla 1) todos los ARNg son objetivo para una secuencia conservada de Mcl-1. (Figura 13-14)

El plásmido PX458 contiene dos casetes de expresión, hSpCas9 y el ARN guía quimérico. El vector se puede digerir usando BbsI, y un par de oligos recocidos (el diseño se indica a continuación) se puede clonar en el ARN guía. Los oligonucleótidos se diseñan basándose en la secuencia del sitio diana (20 pb) y deben estar flanqueados en el extremo 3 'por una secuencia PAM NGG de 3 pb. (Figura 9)

Mcl-1 es un miembro de la familia Bcl-2 antiapoptótico único en el sentido de que su ablación genética da como resultado deficiencias autónomas celulares en una gran cantidad de linajes celulares (Beroukhim et al., 2010). Sin embargo, la ablación del gen Mcl-1 desactiva tanto su actividad antiapoptótica como su capacidad para facilitar la función mitocondrial dentro de la matriz. Por esa razón, será importante determinar las contribuciones relativas de los diferentes roles funcionales de Mcl-1 para promover la supervivencia y el desarrollo de linajes hematopoyéticos y otros linajes celulares. La

función crítica de Mcl-1 durante estas etapas puede ser meramente apoyar la supervivencia celular antagonizando la apoptosis. Sin embargo, Mcl-1 también puede facilitar la aptitud mitocondrial durante la proliferación celular y la diferenciación cuando se modulan las demandas metabólicas en las mitocondrias.

Mcl-1 es uno de los genes más altamente amplificados en una variedad de cánceres humanos (Beroukhim et al., 2010). Como resultado, la mayoría de las estrategias terapéuticas se han dirigido a antagonizar la actividad anti-apoptótica Mcl-1 que intenta fomentar la muerte celular maligna. Sin embargo, estos hallazgos aumentan la posibilidad de que la función no apoptótica de Mcl-1 también pueda alimentar la función mitocondrial en células cancerosas, facilitando así la generación de sustratos derivados mitocondriales requeridos para mantener los niveles de síntesis biomolecular que conducen a la hiperproliferación (Deberardinis, Sayed, Ditsworth y Thompson, 2008). Por lo tanto, la inhibición de la capacidad de Mcl-1 para promover la función mitocondrial puede representar un nuevo objetivo terapéutico en las células cancerosas. (Figura 16-17).

En este estudio, se realizaron varios experimentos para especificar el papel de la sobrecarga de colesterol. Los datos de microarreglos se normalizaron primero utilizando el algoritmo de normalización de cuantiles. Como se muestra, este método de normalización corrigió variaciones técnicas putativas entre muestras. Sin filtración génica inicial, el análisis de componentes principales (PCA) utilizando los valores de expresión de todos los genes en las 24 muestras, principalmente separó el colesterol

de las muestras sin colesterol. Luego, se aplicó una filtración por "bandera" e "intensidad de señal". Se conservaron solo las entidades en las que al menos el 50% de los valores en cualquiera de las dos condiciones. Para la filtración por intensidad de señal, se conservaron las entidades en las que al menos el 50% de los valores en cualquiera de las dos condiciones estaban dentro del rango de interés. Los genes expresados diferencialmente se identificaron mediante una prueba t univariada de dos muestras y un modelo de varianza aleatoria. Como informe anterior (Sulpice et al., 2016)

Uno de nuestros principales intereses fue abordar el perfil de expresión génica inducida por la sobrecarga de colesterol, la desregulación indujo 318 genes, indicando un impacto prominente en la expresión génica que tiende a una respuesta adaptativa, que podría estar relacionada, entre otros procesos fisiológicos, con la resistencia a la apoptosis en un mecanismo que involucra la homeostasis y la función de las mitocondrias, estrechado vinculado a cambios en el estado redox de las mitocondrias.

De acuerdo con nuestros hallazgos previos en un modelo de HCC en ratones (Enríquez-Cortina et al., 2017), trabajos anteriores informamos que bajo dieta HC, y en presencia de un estímulo carcinogénico, los ratones desarrollan un fenotipo agresivo de HCC (Enríquez - Cortina et al., 2017), correlacionando con los datos transcriptómicos actuales; curiosamente, la sobrecarga de colesterol tiene un gran impacto en algunos procesos como proliferación, migración, ruta metabólica, estado

redox. (Domínguez-Pérez et al., 2016; Enriquez-Cortina et al., 2017; Nuno-Lambarri et al., 2016).

Conclusión

En resumen, la sobrecarga de colesterol induce la sobrexpresión de Mcl-1, esta sobreexpresión parece ser específica de la isoforma antiapoptótica, además esta isoforma tiene una estrecha relación en las vías metabólicas. Estos datos apoyan firmemente la premisa de que la sobrecarga de colesterol acelera el proceso de carcinogénesis, y una de las formas es sobre expresar proteínas antiapoptóticas como Mcl-1, que además de proteger la célula contra la apoptosis, también contribuyen al desarrollo de la transformación celular a través de la modulación de las vías metabólicas.

Abstract.

Cholesterol overload in the liver rising a complex response in hepatocytes characterized by mitochondria dysfunction and oxidative stress but, interestingly, hepatocytes with cholesterol overload seems to be resistant to cell death under unstimulated conditions

The results suggest that cholesterol has a direct effect on the level of cellular aggressiveness, the cell migration assays confirm that cholesterol favors the migration of Huh-7 cells, on the contrary the elimination of cholesterol is reflected in the decrease of cholesterol. the migration, likewise it was observed that the cholesterol overload increases the amount of reactive oxygen species (ROS) and likewise an increase in the protein content of Mcl-1 was observed. Given these results we can say that the non-antiapoptotic functions of Mcl-1 play an important role in the progression of HCC since Mcl-1 seems to be a modulator of energy metabolism in Huh-7, likewise cholesterol overload it is a determinant factor for the progression of HCC. The cholesterol overload increases tumorigenic parameters characteristic of the transformed cells.

The participation of Mcl-1 in cholesterol overload is a determining factor for the understanding of molecular mechanisms that could serve as early or preventive markers for HCC.

Abbreviation.

(HCC) Hepatocellular carcinoma

(ASH) Alcoholic steatohepatitis

(NASH) Non-alcoholic steatohepatitis

(NAFLD) Non-alcoholic fatty liver disease

(TG) Triglycerides

(FFA) Free fatty acids

(ASH) Alcoholic steatohepatitis

(LDL) Low-density lipoproteins

(ER) Endoplasmic reticulum

(Stard) Steroidogenic acute regulatory protein, mitochondrial

(ROS) Reactive oxygen species

(mGSH) Mitochondrial glutathione

(H2O2) Hydrogen peroxide

(SOD2) Peroxide dismutase

(BH) Homologous Bcl-2

(BCL-2) B-cell lymphoma 2

(Bcl-xL) B-cell lymphoma-extra large

(MCL-1) Myeloid cell leukemia 1

(BIM) Bcl-2-like protein 11

(BAX) BCL2 Associated X

(NIH) National Cancer Institute of the United States

(PBS) Phosphate-buffered saline

(Cx) Complex Cholesterol-Ciclodextrin

(Cdx) Cyclodextrin

(OPA) O-phthalaldehyde reagent

(DCFDA) Dichlorofluorescin diacetate

(DHE) Dihydroethidium

(qRT-PCR) Quantitative reverse-transcription polymerase chain reaction

(GFP) Green protein florescence

(gRNA) guide RNA

(OCR) Oxygen Consumption Rate

(ECAR) Extracellular Acidification Rate

(T) Tumors

(ST) Surrounding tissue

(DSBs) Double-stranded breaks

(mRNA) Messenger RNA

(DEN)

(GSEA) Gene set enrichment analysis

Index.

Figures Index.

Introduction.

The hepatocellular carcinoma.

The hepatocellular carcinoma (HCC) is the most common primary tumor in the liver. The overall incidence of primary cancer in the liver has progressively increased during the last decades (He et al., 2017). Among the malignant neoplasms of the liver, the hepatocellular carcinoma is the most prevalent, affecting about one million individuals annually worldwide, with an incidence of 500,000 to 1,000,000 cases, the mortality rate is approximately equal to its incidence while, that nationally chronic liver diseases occupy the fourth place of the main causes of mortality. On the other hand, in the population of productive age (15-64 years) they occupy the second place, with the importance of liver diseases as public health in Mexico problems being evident. (http://www.dgis.salud.gob.mx/contenidos/sinais/e_mortalidadgeneral.html).

Generally, among the different types of primary hepatic neoplasms such as cholangiocarcinoma (epithelial cell bile duct cancer), hepatoblastom (malignant liver tumor in early childhood), HCC deserves special mention given its high level of incidence (Dutta & Mahato, 2017). Multiple risk factors for the development of HCC have been related, such as chronic infection with hepatitis B and C viruses, alcohol abuse, the presence of diabetes, nonalcoholic steatohepatitis (NASH) and metabolic syndrome, among others. (Enriquez-Cortina et al., 2017).

Non-alcoholic fatty liver disease.

Non-alcoholic fatty liver disease (NAFLD) was described (Ludwig, Viggiano, McGill, & Oh, 1980) as a morphological pattern of liver injury in patients mainly with obesity and

diabetes mellitus, in which there is no history of alcohol consumption and / or abuse, which histologically show changes similar to those observed in alcoholic steatohepatitis (ASH) (Liu, Baker, Bhatia, Zhu, & Baker, 2016). It is considered that the lipid overload in the 5% of hepatocytes leads to NAFLD.

NAFLD can progress to fibrosis, cirrhosis or directly to HCC, (Enriquez-Cortina et al., 2017) non-alcoholic liver diseases are subdivided NAFLD and NASH. Steatosis occurs without evidence of inflammatory process in NAFLD. If the aggressor agent is maintained, it will evolve to NASH (which is associated with liver inflammation), histologically indistinguishable from alcoholic steatohepatitis (Bellentani, 2017). Currently, NAFLD is considered a hepatic component of the metabolic syndrome. One of the most important risk factors is the histological evidence of inflammation (Singh et al., 2015).

In the first stage of steatosis the liver, the combination of genetic and acquired factors contributes to the accumulation in excess of triglycerides (TG) and fatty acids. The mechanisms that potentially contribute to the accumulation of lipids in the hepatic parenchyma are the high flow of non-esterified fatty acids to this organ, the increase in de novo hepatic lipogenesis, decrease in beta oxidation of free fatty acids (FFA). and the alteration in the incorporation of TG in very low density lipoproteins (VLDL) or in the secretion of said lipoproteins (Liu et al., 2016).

Cholesterol and liver disease.

The role of cholesterol in steatohepatitis has attracted increasing attention in recent years and is currently considered a key factor in ASH and NASH. (Enriquez-Cortina et al., 2013)Although the pathogenesis of these diseases is different they have indistinguishable histological characteristics and common underlying mechanisms.(Gomez-Quiroz et al., 2008)

The synthesis of cholesterol is restricted to a subset of tissues such as liver and adipose tissue mainly. The reactivation of the biosynthesis of lipids and cholesterol has been observed frequently in HCC (Ikonen, 2008).

Hypercholesterolemia is the factor that presents the highest risk for cardiovascular diseases, it has been positively correlated with the incidence and mortality of coronary disease, however, until a few years ago, its specific contribution in the progression of liver damage had been little studied (Zafrir et al., 2017).

Cholesterol is an essential constituent in biological membranes, which plays a key role in the physiological properties and in the regulation of signaling pathways. Due to the regulation, it exerts on the fluidity of the membranes. Cholesterol is an important determinant in the relative permeability of the lipid bilayer and is heterogeneously distributed between the membranes (Ribas et al., 2016).

Cholesterol induces the packaging of the membrane in specific microdomains of the plasma membrane, providing a platform for a variety of signaling proteins associated with the membrane (Ribas, Garcia-Ruiz, & Fernandez-Checa, 2014). Not all cellular

bilayers present in their composition the same cholesterol levels, this is particularly abundant in the plasma membrane (Ikonen, 2008).

In addition to these essential functions of cholesterol, cells satisfy their cholesterol needs from different sources and mechanisms, including uptake by low-density lipoproteins rich in cholesterol (LDL) (Hwang et al., 2016), and the synthesis of Novo from acetyl-CoA in the endoplasmic reticulum (ER). Once synthesized, cholesterol is distributed to other membranes including that of the mitochondria (Garcia-Ruiz et al., 2009). The mitochondria, in addition to generate energy for the cell, plays an important role for some pathways of cell death, such as apoptosis (dependent and independent of caspases). The accumulation of cholesterol in the mitochondria decreases the fluidity of the mitochondrial membranes, which increases the threshold of permeabilization of the mitochondrial outer membrane by restructuring the mitochondrial membrane bilayers, (Ribas et al., 2016) the accumulation of mitochondrial cholesterol it can contribute indirectly to the metabolic changes of cancer cells by the deterioration of mitochondrial function and the activation of survival programs (Maierean et al., 2017).

The emerging evidence points to the small accumulation of mitochondrial cholesterol as a key factor in several diseases prevalent in humans, including the transition from steatosis to steatohepatitis and its progression to HCC.(Nuno-Lambarri et al., 2016)

Since the role of cholesterol in the regulation of physiological properties, membrane dynamics, as well as signal transduction, synthesis and supply of cholesterol in the membrane are highly regulated processes.

Non-esterified cholesterol is located mainly in the plasma membrane where specific domains are formed. (Rosales-Cruz et al., 2018)The transport of mitochondrial

cholesterol is preferably carried out by Stard1, which regulates the transport of cholesterol from the outer membrane to the inner mitochondrial membrane, thus contributing to the regulation of cholesterol levels in the membrane to prevent its accumulation(Lopez-Islas et al., 2016). Any deregulation in these mechanisms can generate adverse effects on the function such as loss in membrane integrity, fluidity of the membrane, signaling and cell communication (Garcia-Ruiz, Ribas, Baulies, & Fernandez-Checa, 2016).

Cancer cells exhibit critical metabolic changes induced by mutations, which cause an increase in the oncogenes function and the loss of function of tumor suppressor genes. This results in alteration in cell metabolism, growth deregulation, resistance to cell death, invasion and metastasis (Hanahan & Weinberg, 2011). Many of these characteristics are regulated by changes in mitochondrial function and, perhaps, by changes in cholesterol metabolism, as well as their transport to the mitochondria.(Gomez-Quiroz et al., 2016)

Oncogenic transformation requires a reprogramming of energy metabolism to support growth without restrictions. Mitochondrial dysfunctions have been implicated in a wide variety of human pathologies, including cancer and age-related diseases (Wallace, 2005). The growing evidence indicates that mitochondrial dynamics have roles beyond the maintenance of morphology and the impact on cell death and metabolism (Chen & Chan, 2005). Experimental evidence indicates that the increase in cell proliferation and

tumor growth are closely related to the increase in cholesterol requirements (Dang, 2012).

The mitochondria.

The mitochondria are one of the main sources of reactive oxygen species (ROS) (Gomez-Quiroz et al., 2016)(Venditti et al, 2013), so an effective antioxidant system is required. Mitochondrial glutathione (mGSH) is a central component, prevents or repairs the oxidative damage generated during normal aerobic metabolism (Ribas, Garcia-Ruiz, & Fernandez-Checa, 2014). The primary generation of ROS in the mitochondria is the superoxide anion, which is produced in the mitochondrial matrix, which can be dismuted into hydrogen peroxide (H2O2). This reaction is catalyzed by its peroxide dismutase (SOD2) (Mari et al., 2010). The series of events that lead to apoptosis have been categorized into two modes, the extrinsic and intrinsic apoptotic pathways (Li & Dewson, 2015). The anti-apoptotic proteins of the Bcl-2 family are formed by several homologous domains (BH1 to BH4), especially the BH3 domain allows them to bind to other proteins of the same family. Among the most important proteins of this family are Bcl-2 Bcl-xL and myeloid cell leukemia 1 (Mcl-1), their location is generally mitochondrial but they have also been found in the endoplasmic reticulum and in the nuclear membrane (Li & Dewson, 2015).

Mcl-1.

Mcl-1 is a pro-survival member of the Bcl-2 family which was initially identified as an early expression gene during the differentiation of myeloid leukemia cells (Elgendy et al., 2017). Algorithms of alignment identified similarity in the protein sequence of

survival of Bcl-2, for that reason when it was discovered Mcl-1 constituted the second member of this family of proteins (Elgendy & Minucci, 2015). The Bcl-2 family has been considered a new class of genes that promote oncogenesis, although not through the positive regulation of proliferation, but maintaining viability through the inhibition of apoptosis (Schwickart et al., 2010). The deregulation of the expression and function of the Bcl-2 family of proteins has been implicated since then in all neoplasias(Zhen et al., 2017).

A sequential analysis revealed that while Mcl-1 contained three putative BH domains, and could experimentally protect against apoptosis, its N-terminal region contains potential regulatory motifs that could regulate its function (Thomas, Lam, & Edwards, 2010). Mcl-1 is different from its pro-survival family because it has a larger size of 350 residues, greater than the 239 of Bcl-2. Residues 170-300 of Mcl-1 share a large amount of structural and functional homology with Bcl-2, which contains its three BH domains (Bcl-2 possesses 4 domains), which confer the ability to heterodimerize with other members of the family (Day et al., 2005).

The increase in the expression of Mcl-1 can contribute to cancer, in fact, alterations in the expression of Mcl-1 as occurs in other proteins of this family, serve as indicators of response to the disease in patients with cancer: for example, a high expression of Mcl-1 is associated with an accelerated progression of the disease, as well as a decrease in the response to therapy Mcl-1 blocks the progression of apoptosis by binding and sequestration of pro-apoptotic proteins Bim and Bax, that are capable of forming pores in the mitochondrial membrane allowing the release of cytochrome c in the cytoplasm

and inducing the activation of caspases responsible for much of the macromolecular degradation observed during apoptosis (Thomas et al., 2010).

Justification.

The evolution of NAFLD to HCC is a slow process, which can take up to 30 years, so specific data on the HCC fatty liver ratio do not exist at the moment. Currently, the increase in the consumption of foods with high caloric content is causing an increase in obesity and metabolic syndrome. It is known that Mexico ranks second in adult obesity worldwide and the first in childhood obesity (Aceves-Martins, Llaurado, Tarro, Sola, & Giralt, 2016). Given the above data it is easily predictable that in the next 20 years there will be an alarming increase in cases of HCC, being more worrying the fact that it can occur at much younger ages. Recently the National Cancer Institute of the United States (NCI / NIH), reported in its "Annual report to the nation on the status of cancer, 1975-2012" (Ryerson et al., 2016), that the general mortality by cancer is decreasing significantly, however, four neoplasms are increased far from decreasing, with the liver having the greatest increase (which in itself represents an international alert).

Previous data in our laboratory the general aim of the work(Enriquez-Cortina et al., 2017) was to address the oxidative stress-mediated DNA damage induced by cholesterol overload, and its role in the development of hepatocellular carcinoma. In this paper (Dominguez-Perez et al., 2016) we aimed to figure out the protective effect of this growth factor in hepatocytes overloaded with free cholesterol The aim of this paper (Nuno-Lambarri et al., 2016) was to investigate the impact of liver cholesterol

overload on the progression of the obstructive cholestasis in mice subjected to bile duct ligation surgery. Furthermore, we describe the effect of low cadmium acute treatment on hepatocytes obtained from mice fed with a high cholesterol diet. Our data suggest that hepatocytes with cholesterol overload promote an adaptive response against cadmium-induced acute toxicity by up-regulating anti-apoptotic proteins, managing ROS overproduction, increasing GSH synthesis and MT-II content to avoid protein oxidation (Rosales-Cruz et al., 2018) On the other hand, we evaluated the effect of ethanol and acetaldehyde on primary hepatocytes obtained from mice fed for two days with a high cholesterol (HC) diet. HC hepatocytes increased lipid and cholesterol content. HC diet sensitized hepatocytes to the toxic effect of ethanol and acetaldehyde (Lopez-Islas et al., 2016)show that both cholesterol and lipid overload are associated with a poor prognosis in HCC; in fact, gene overexpression of proteins related to lipogenesis shows a more aggressive phenotype in HCC. The increase in markers of tumorigenicity, such as proliferation, are up-regulated, indicating a deregulation in anti-apoptotic proteins such as Mcl-1. So, understanding the role that Mcl-1 plays in HCC is of paramount importance.

Research question.

Which is the role of Mcl-1 in cholesterol overloaded human hepatocellular carcinoma cell line?

Hypothesis

Cholesterol overload in Huh7 cell line will increase the aggressiveness phenotype in a mechanism driven by Mcl-1 overexpression.

General Aim

Determine the relationship between cholesterol overload and Mcl-1 expression with cellular malignancy parameters in the human HCC cell line Huh7.

Particular Aims

1.- Determine if the cholesterol overload have relation with the Mcl-1 expression in tumor cells.

2.-Determine if Mcl-1 Increases malignant cells parameters in environment with cholesterol overload.

3.- Characterize the mechanism by the cholesterol overload induces overexpression of Mcl-1.

4.-Characterize tumorigenic parameters in hepatocarcinoma cell lines by Mcl-1 silencing or overexpression whit cholesterol overload.

Experimental Design

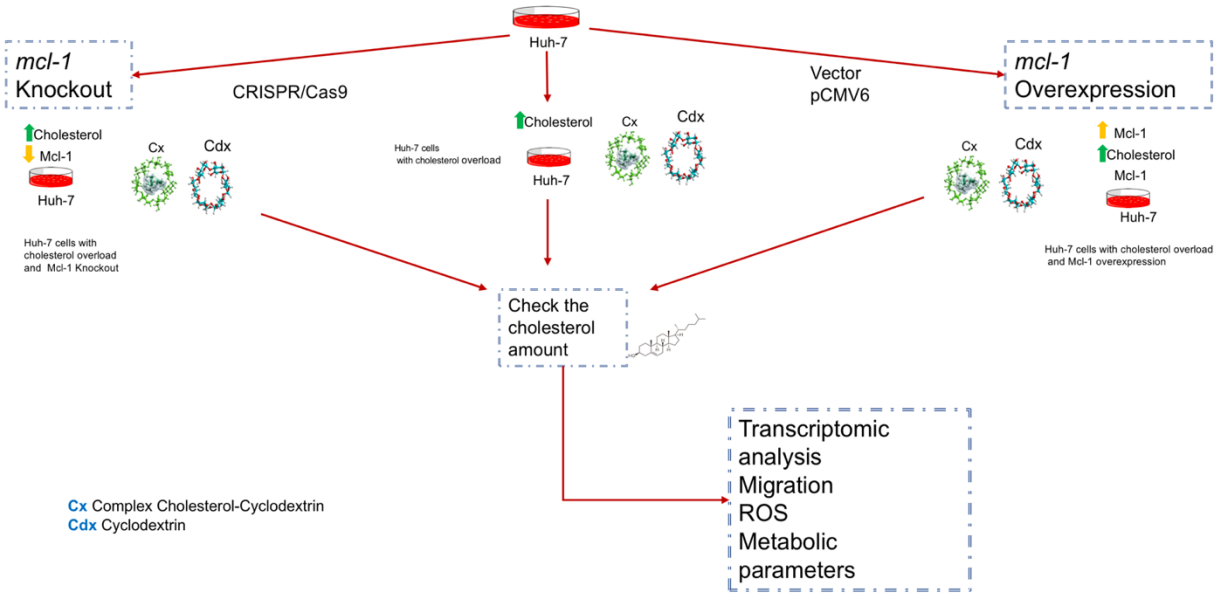

Materials and methods

Cell culture: Human HCC cell Huh7 line was obtained from ATCC.

Cell lines were seeded at 48 000 cells/cm^2 in Petri dishes (Corning, USA) using Williams' E medium for Huh7, supplemented with 10% (v/v) fetal bovine serum (FBS, Hyclone Laboratories Inc., Logan Utah, USA). The cells were incubated at 37 °C (5% CO2 and 95% air at saturation humidity) and checked for adherence of monolayer after 4 h. Once adhered, the cells were washed with phosphate-buffered saline (PBS) and the medium was replaced for a serum-free growth medium. The following 4 h, cells were treated with Complex Cholesterol-Ciclodextrin (Cx) and Cyclodextrin (Cdx) for 90 min. Cholesterol and Cdx were purchased from Sigma.

Animals: Sixty 14-days old male mice (C57/BL6) were randomly separated in four groups: fed with a high cholesterol diet (HC, 2% cholesterol and 0.5% sodium cholate); HC diet and a single intraperitoneal injection of 10μg/g body weight of DEN (Sigma-Aldrich); control animals received regular Chow diet (CW) with or without DEN as previous reported in (Enriquez-Cortina et al., 2017)

Mice were euthanized and serum and liver tissue were examined at 8 months. All animals were maintained in specific pathogen-free housing and cared in accordance with the NIH Guide for the Care and Use of Laboratory Animals. (Enriquez-Cortina et al., 2017)

Western blot analysis: Western blot analysis was performed as described in previous studies by our group (Enriquez-Cortina et al., 2017). Cells were lysed with M-PER Mammalian protein extraction reagent (Thermo scientific) supplemented with proteases inhibitor and phosphatases inhibitor COMPLETE and phosSTOP respectively (Roche Diagnostics, Barcelona, Spain) and centrifuged at 12,879g for 15 min at 4℃. The supernatants were collected and the protein concentrations were determined with a bicinchoninic acid assay kit (Pierce™ BCA protein assay kit, Thermo scientific). The protein (80μg/ml) was subjected to 10% SDS-PAGE and transferred to low fluorescence 0.2μm PVDF membranes (GE Healthcare Life Sciences). After blocking with 5% nonfat milk at 4℃ for 2 h, the membranes were probed with primary antibodies against the analyte proteins stated above (1:1000 dilution) and β-actin (1:10,000 dilution) at 4℃ overnight. Following three washes with PBS, the membrane was incubated with secondary antibody at room temperature for 2h horseradish peroxidase conjugated and was used according primary antibodies. Blots were revealed using luminol. Protein bands were scanned and the band intensities quantified using a densitometer Imaging System (Gel Logic 1500, Kodak).

Wound Healing Assays: As reported by (Jimenez-Salazar et al., 2014), Huh-7 cells were grown to 100 % confluence. Cells were maintained in culture medium for 24 h before “wounding” (scratching), and then treatments (Cx160μg/ml, Cdx10mM) were supplemented to wells during 4, 12, 24, or 48 h. Linear scratches (approximately 0.7-mm wide) were gently made with a sterile pipette tip across the culture surface; wells

were then rinsed with PBS to remove debris. In order to show that wound healing is due to cell migration instead of Cx-induced cell proliferation, cells were also incubated in the absence and presence of 10 μM cytosine β-d-arabinofuranoside hydrochloride, a DNA synthesis inhibitor, at 48 h of Cx incubation. For each condition, at least five pictures were taken with an inverted microscope (Carl Zeiss Axiovert 40 CFL) at 0, 4, 12, 24, and 72 h after scratching. The proportion of unrecovered wound area was calculated by dividing the unrecovered area after cholesterol treatment with the initial wound area at 0 h

Free cholesterol determination by filipin staining and quantification: Cells were fixed with PFA 4% for 15 minutes at room temperature. For free cholesterol determination, cells were incubated with filipin as previously reported (Rosales-Cruz et al., 2018). After 3 final washes in PBS, cells were mounted and confocal (NLO780 Carl Zeiss) microscopy images were collected using UV light excitation. The quantification of free cholesterol was assessed using the Total Cholesterol Assay Kit (Cell Biolabs, Inc., San Diego CA, USA) following the manufacturer instructions.

Cholesterol Determination: $2x10^6$ cells in 200μL of PBS was saponified with alcoholic KOH in a 60ºC heating block for 15 min. After the mixture had cooled, 2mL of hexane and 600μL of distilled water were added and shaken to ensure complete mixing. Appropriate aliquots of the hexane layer were evaporated using SpeedVac concentrator and used for cholesterol measurement with O-phthalaldehyde reagent

(OPA) (Sigma-Aldrich) dissolved in acetic acid; after that sulfuric acid was added and then read at 550nm in the spectrophotometer. as previously reported (Dominguez-Perez et al., 2016).

ROS determination: The cells were incubated at 37 °C (5% CO2 and 95% air at saturation humidity) and checked for adherence of monolayer after 4 h. Once adhered, the cells were washed with PBS and the medium was replaced for a serum-free growth medium. Cells were treat with Cx and Cdx for 90 min, and the plates were immediately incubated for 15 min, in the dark, at room temperature with either 2',7' – dichlorofluorescin diacetate (DCFDA, 5 μM), a cell-permeable non-fluorescent probe that is intracellularly de-esterified and converted to the highly fluorescent 2′,7′-dichlorofluorescein (DCFH) upon oxidation by ROS, particularly peroxides, or with dihydroethidium (DHE, 1 μM) for determination of superoxide anion radical detecting ethidium fluorescence. Samples were covered and observed using a confocal microscope at excitation and emission wavelengths of 480 and 520 nm, respectively, for DCFDA; and excitation and emission wavelengths of 485 and 570 nm, respectively, for DHE- derived ethidium fluorescence, as we previously reported (Nuno-Lambarri et al., 2016).

***mcl-1* expression:** Quantitative reverse-transcription polymerase chain reaction (qRT-PCR): was performed as described (Coulouarn et al., 2012) Total RNA was isolated using Qiazol Reagent (Thermo Fisher Scientific). And was purified with an miRNAeasy kit(Qiagen). One μg of total RNA was subjected to reverse transcription using a SYBR Green master mix (Applied Biosys-tems, Carlsbad, CA). A mixture of

deoxythymidineoligomer (250 ng) and random hexamers (100 ng) wasused to prime the RT reaction of 1mg total RNA (Superscript III RT; Invitrogen)

green Supermix (Bio-Rad), reactions were run in Bio-Rad CFX96 Touch Real-Time PCR detection system (Bio-Rad).

Gene expression profiling: Total RNA, including lncRNA and micro RNA (miRNA, miR), was purified with an miRNAeasy kit(Qiagen). Genome-wide expression profiling was performed using the low-input QuickAmp labeling kit and human SurePrint G3 8x60K probes pangenomic microarrays (Agilent Technologies, Santa Clara, CA) as described. (Coulouarn et al., 2012) These microarrays include 26,083Entrez genes and 30,606 lncRNAs. Gene expression data were processed using Feature Extraction and GeneSpring software (Agilent Technologies). Gene set enrichment analysis (GSEA) was performed using the Java tool developed at the Broad Institute (Cambridge,MA). The Enrichr algorithm (http://amp.pharm.mssm.edu/Enrichr) was also used to identify key genes associated with relevant signaling pathways.

The plasmid PX458. was obtained from Addgene (# 48138, 32), it has an ampicillin resistance gene for selection in bacteria, it also contains the sequence of the hSpCas9 gene of S. pyogenes linked to the Green protein florescence (GFP) gene by the peptide 2A sequence for co-production of both proteins, the expression of both genes is directed by a synthetic CAG promoter. In addition, the plasmid contains the sequences necessary for the expression of the guide RNAs.

NAME	SEQUENCE 5'→3'	SIZE	% GC	TM
gRNA1 **F**	CAC CGA GGC GCT GGA GAC CTT ACG A	**25**	**64.0**	**65.9**
gRNA1 **R**	AAA CTC GTA AGG TCT CCA GCG CTT C	**25**	**56.0**	**62.4**
gRNA2 **F**	CAC CGC CAA AAG TCG CCC TCC CGG G	**25**	**72.0**	**69.7**
gRNA2 **R**	AAA CCC CGG GAG GGC GAC TTT TGG C	**25**	**64.0**	**67.6**
gRNA3 **F**	CAC CGG AAG AAA AGC AGC CTC GCA G	**25**	**64.0**	**66.0**
gRNA3 **R**	AAA CCC GCG AGG CTG CTT TTC TTC C	**25**	**56.0**	**63.9**

Cloning protocol: The vector can be digested using BbsI, and a pair of annealed oligos (design is indicated below) can be cloned into the guide RNA. The oligos is designed based on the target site sequence (20bp) and needs to be flanked on the 3' end by a 3bp NGG PAM sequence as previously reported (Ophinni, Inoue, Kotaki, & Kameoka, 2018)

The vector constructs were sequence-verified using primers PX458F and PX458R (see supplementary Table 1) and Big-dye terminator sequencing kit 3.1 (Applied Biosystems®,USA). Sequences provided by the 3130x1 Genetic Analyzer (Applied Biosystems®, USA) were obtained, alignment and consensus sequences were obtained using the SeqScape program (ABI Prism ® version 2.1, USA). For this study, we continued with those constructs in which guide RNA (gRNA) sequences.

NAME	SEQUENCE 5'→3'	SIZE	% GC	TM
PX458 F	GGGCCTATTTCCCATGATTCC	21	52.4	55.7
PX458 R	GCGCTAAAAACGGACTAGCC	20	55	56.5

Table1 Primers used to verify gRNAs sequences inserted in PX458 plasmid

Transformation: A vial with 100µl of ultracompetent E. coli cells was taken and mixed with 1µl of vector or, 10µl of the ligation mixture. The conditions of

Heat shock transformation of E. coli from the STABLE strain were as follows. The mixture was incubated for 30 min at 4ºC and 2 min at 42ºC. Subsequently, the cells were incubated for 1 h at 38°C at 150 rpm. They were seeded on LB plates supplemented with Kanamicyn (100µg / ml) overnight at 37oC as described

The reaction was incubated 30 min at 4oC and 2 min at 42oC. Subsequently, the mixture was incubated for 1 h at 38 ° C with stirring in 1 ml of liquid LB medium. Once the time was passed, it was planted in LB medium and incubated overnight at 37oC. This for the production of the vector

Transfection: The plasmids were transfected using Lipofectamine 2000 (Invitrogen, Carlsbad, CA), following the manufacturer's instructions. For the visualization of reporter proteins GFP in the Carl Zeiss LSM 780 NLO confocal microscope (Carl Zeiss, Inc., USA), 100 ng of plasmid was used. as described

Determination of Oxygen Consumption Rate (OCR) and Extracellular Acidification Rate (ECAR) by Seahorse technology.

In vivo real-time OCR and *Extracellular Acidification Rate* (ECAR) were monitored by the Seahorse XF24 Flux Analyzer (Seahorse Bioscience) according to the manufacturer's instructions. Huh-7 cells were seeded at 50,000 cells/well density in 24-well plates for 1 h in complete DMEM (10% FBS, 1% P/S) to allow adherence to the plate. For assessment of the real-time ECAR, cells were incubated with unbuffered assay media (XF Media Base containing 2 mM L-Glutamine) followed by a sequential injection of 10 mM glucose, 2 µM oligomycin and 50 mM 2-deoxyglucose. For OCR cells were incubated with unbuffered assay media (XF Media Base with 25 mM glucose, 4 mM L-glutamine and 5 mM pyruvate) followed by a sequential injection of 2µM oligomycin, 0.2 µM carbonyl cyanide 4-(trifluoromethoxy) phenylhydrazone and 2 µM antimycin A plus Rotenone. Both ECAR and OCR measurements were normalized to ug of total protein following Bradford protein assay. as previously reported (Baulies et al., 2018)

Statistical analysis*:* The data are presented as mean ± S.E. for at least three independent experiments carried out by triplicate. Comparisons between groups were made using ANOVA test with a Tukey post-hoc analysis. Differences were considered significant at $p < 0.05$. The Prism software version 6 was used to run the analysis.

Results.

Validation of cholesterol incorporation stability and localization.

To begin with, the in vitro model of cholesterol incorporation into cells derived from liver cancer was validated (Figure 1a) shows an increase in the cholesterol content in the Huh-7 cells treated with the Cx for 90 min, this increase represents 10-times more cholesterol content than the untreated cells, on the other hand, the cells treated with Cdx show a decrease in the amount of cholesterol compared to the untreated ones, it is important to mention that the impact of cholesterol overload in the in vitro form, must represent physiological values as reported (Rosales-Cruz et al., 2018). We use HepG2 cell line just to validate, that the incorporation of the cho was not exclusively for Huh-7 cell line (Figure 1b).

Experiments were also carried out in primary mouse hepatocytes fed a chow diet, to corroborate that the model not only worked in transformed cells, but could also be used in cells without some type of mutation, so cells were treated with 160μg/m Cho and Cdx for 90 min respectively, and it was observed an increment of 6-fold compared with control (Figure 1c).

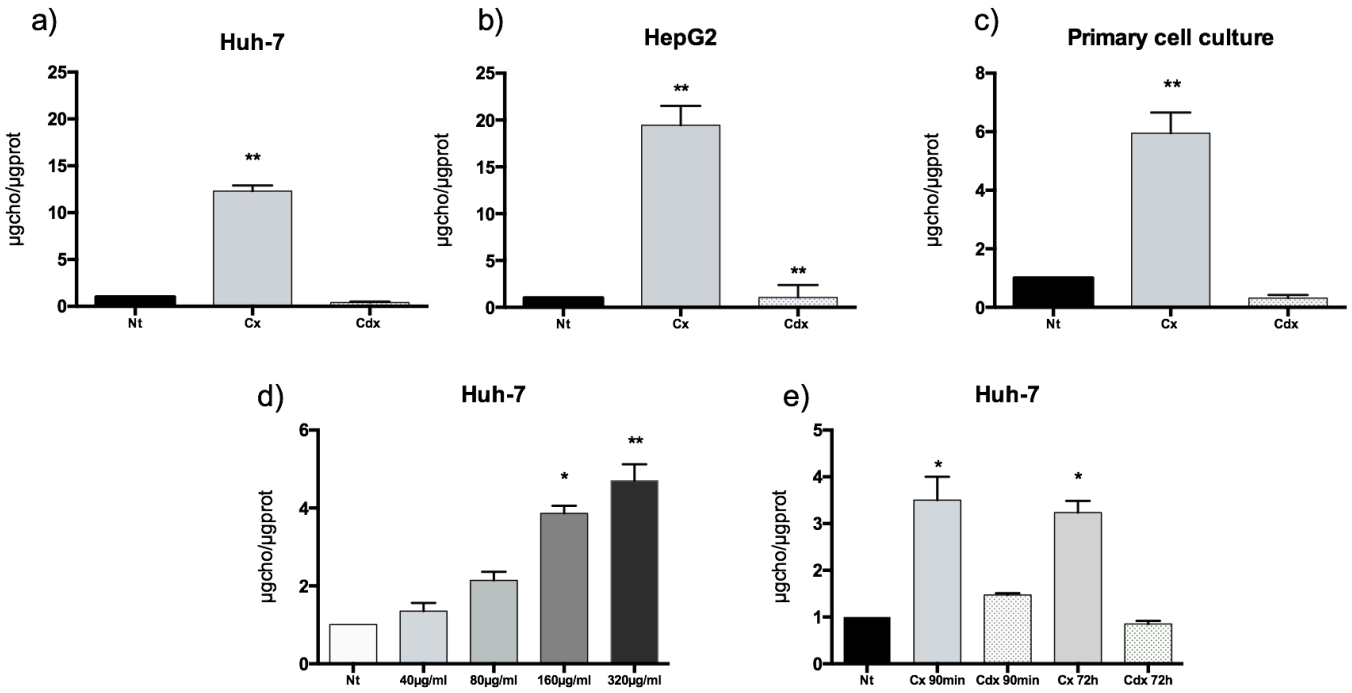

Figure 1. Determination of cholesterol overload. Huh-7 cells were treated with the Cx 400µg/ml and Cdx 10 mM for 90 min **a)** total cholesterol quantification by OPA. **b)** HepG2 cells were treated with the Cx 160µg/ml and Cdx 10 mM for 90 min. **c)** Hepatocyte primary culture was obtained from mice which feded chow diet. **d)** Huh-7 cells were treated with different concentrations of the Cx 160µg was the optimal concentration. **e)** Huh7 the cells were treated with the Cx 90 min. but the quantification was until 72h (first and second bars). Huh7 cells were treated for 72h, the quantification was at 72h (third and fourth bars). Results are expressed in µgcho/µg protein. Each bar represents the mean S.E. of at least three different experiments. * *P<0.05; ** P<0.01; *** P<0.001) vs Nt

To determine a concentration that represented a physiological effect similar to mice fed high-cholesterol diet, different concentrations were used, the concentration that had

similar in vivo effects is 160μg/mL because this increased around 4-5-fold the amount of cholesterol, just like in mice (Figure 1d).

In order to figure out if the cholesterol that was incorporated in the cell line remained inside it along the experimental procedures, cholesterol was determined up to 72 h after its incorporation, in the same experiment the cells were treated for 72 h to figure out the best form of incorporation (Figure 1e).

Filipin staining confirmed the free cholesterol content in Huh-7 and Hep3B cell line increase when cells were treated with the Cx. To address the localization of cholesterol incorporated, mitochondria were labeled with Mitotracker, it can be observed that an important part of the cholesterol loaded was found in mitochondria, now really know our model works, and it´s capable to increase the cholesterol amount, in different cell lines, in this time we use Hep3B (Figure 2).

Cholesterol overload increases cell migration.

In order to evaluate the physiological effects of cholesterol overload, a wound-healing assays were performed, we treated Huh-7 cells with Cx and Cdx. We observed that the cells with the highest amount of cholesterol had a greater ability to close the wound migrating faster comparing to not treated cells (Figure 3). To differentiate that the process was migration rather than proliferation Huh-7 cells were incubated in presence of 10μM cytosine β-D arabinofuranoside hydrochloride for 48 h after the addition of

cholesterol. Similar results were observed in the absence and presence of the DNA synthesis inhibitor. (Jimenez-Salazar et al., 2014)

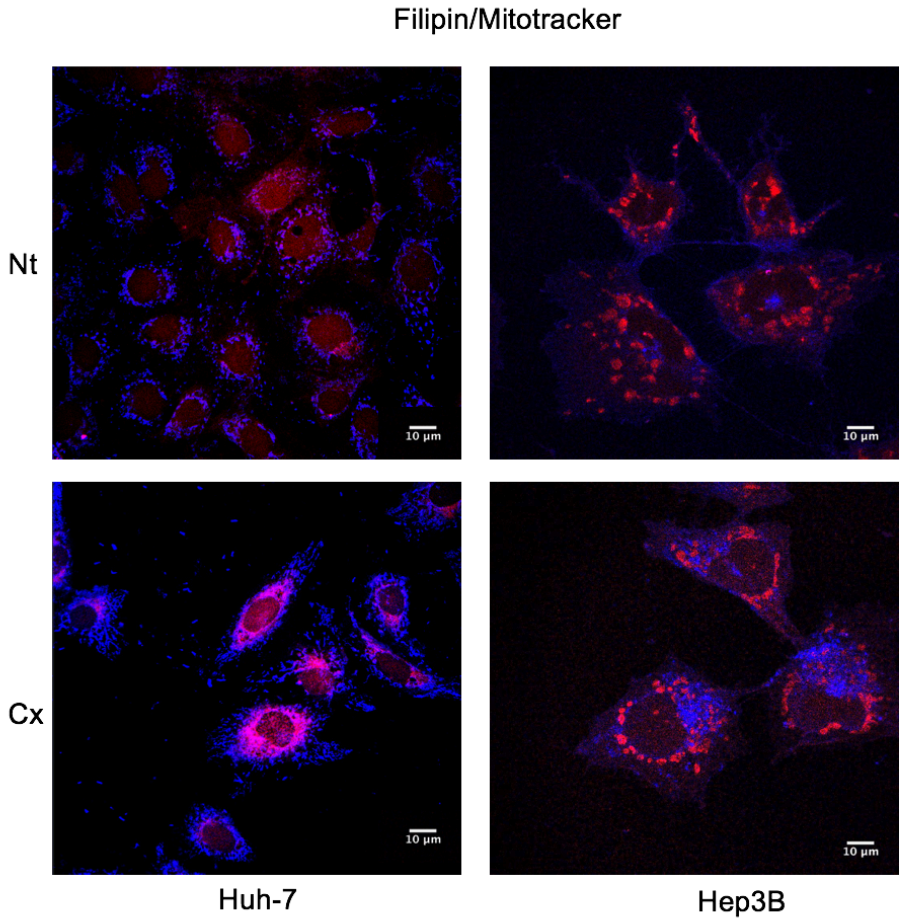

Figure 2. Cholesterol overload distribution. Confocal fluorescence images of Filipin and mitochondrial stain. Huh-7 and Hep3B cells were treated with Cx 160µg for 90 min. the cholesterol is stain in blue and mitochondria in red, the pink color represents match. Images are representative of at least three independent experiments.

The cell migration assays confirm that cholesterol increases cell migration of Huh-7 cells, on the contrary the elimination of cholesterol is reflected in the decrease of cellular

migration. These results suggest that cholesterol could increase cellular aggressiveness.(Lopez-Islas et al., 2016)

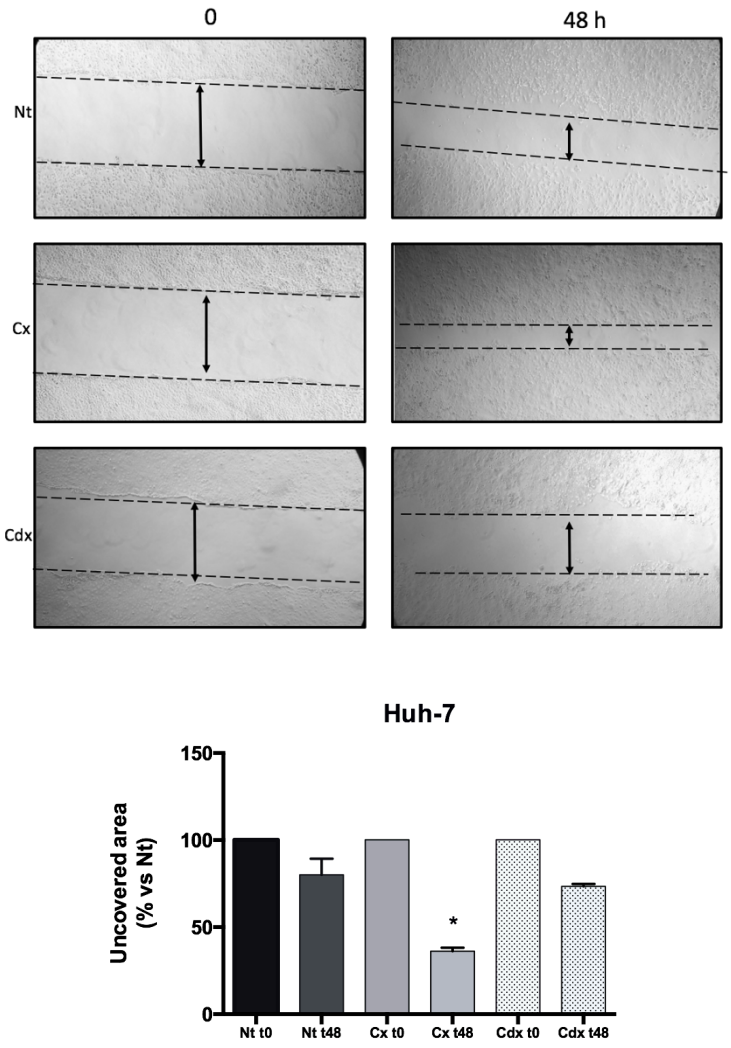

Figure 3. Cholesterol overload induces cell migration. Huh-7 cells are induced by Cx to undergo cell migration. Confluent monolayer of Huh-7 cells were wounded with a uniform

scratch. Experiment was conducted for 0, 4, 12, 24, or 48h of incubation with Nt, Cx and Cdx. Images of cell cultures were captured at 0, 4, 12, 24, or 48 h after scratching, experiments were performed in the absence and presence of the selective inhibitor of DNA synthesis cytosine β-d-arabinofuranoside hydrochloride (10μM) The arrow indicates the wound edge. Images are representative of at least three independent experiments. Each bar represents the mean S.E. of at least three different experiments. * *P<0.05; vs Nt

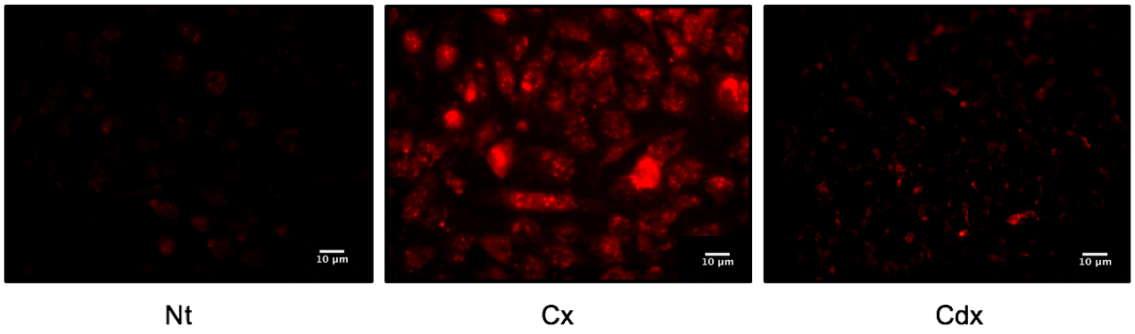

Figure 4. Cholesterol overload induces ROS. DHE fluorescence for superoxide anion. Representative fluorescence microscopy images (200X) Huh-7 cells treated only with cyclodextrin do not increase de ROS, but cells treated with the Cx enhance the ROS. Each image represents at least three different experiments. Images are representative of at least three independent experiments.

Cholesterol overload increases ROS

As previously observed in experimental animals, cholesterol intake from the diet indices ROS production (Gomez-Quiroz et al., 2016). To explore if the same effect is presented in the in vitro mode, ROS content was measured by DHE fluorescence. Cells treated with cholesterol significantly increased ROS. Figure 4 shows the superoxide content is increased by cholesterol overloading at 90 min of treatment, while Cdx did not induce

any change. This increment is consistent with motogenesis results, due to ROS are among the main inducers of motility (Dominguez-Perez et al., 2016).

Cholesterol overload induces overexpression of Mcl-1

Given that cholesterol overload plays a very important role in the induction of cancer (Yu, Liu, Chen, & Lin, 2016), we decided to observe if the cholesterol overload induces the expression of Mcl-1 as well as some proteins of the Bcl2 family such as Bcl2, BclxL. It was found that cholesterol overload induced an increase in the protein content of the anti-apoptotic isoform of Mcl-1 with no effects in the others members of the family, such as BclxL and Bcl2, in the same way cholesterol overload increase Stat3 phosphorylated in ser727, Stat3 is the transcription factor of Mcl-1. (Figure 5a). We corroborated the Mcl-1 result by qRT-PCR, (Figure 5b).

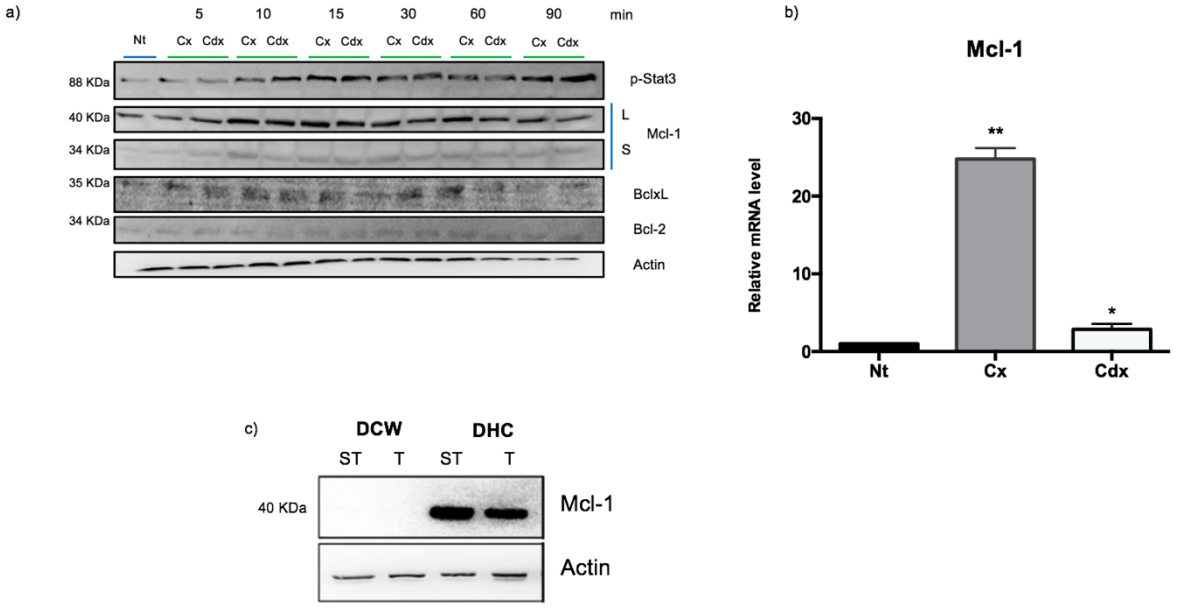

Figure 5. Cholesterol overload induces the expression of Mcl-1 Huh7. **a)** Total protein was isolated from Huh-7 cell line a Western blot analysis of proteins of the Bcl-2 family and p-Stat3 ser727 treated with Cx and Cdx for different times. 5, 10, 15, 30, 60 and 90 min. The image is representative of at least three independent experiments. Actin was used as loading control. **b)** Mcl-1 expression increased by short-time incubation with Cx, Mcl-1 messenger RNA (mRNA) levels were measured in 90 min after treatment. Analysis of MCL-1 expression in Huh-7 cell line. Each column represents the mean ± SEM in at least three independent experiments. *, $p \leq 0.05$, *, $p \leq 0.01$ vs NT. **c)** Total protein was isolated from primary cultured hepatocytes from mice fed with high cholesterol, Western blot analysis of proteins of the Mcl-1. The image is representative of at least three different animals. Actin was used as a loading control.

The relevance on the expression of Mcl-1, particularly in cancer cells, strongly suggest a possible tumor promotion characteristic of cholesterol. To verify this, mice were fed a high cholesterol diet (1% cholesterol) for 3 months and received a single dose of DEN (10μg/g) as carcinogen, as previous reported (Nuno-Lambarri et al., 2016) and the protein content of Mcl-1 was determined in tumors (T) and surrounding tissue (ST), shows that certainly the cholesterol intake increases the expression of this antiapoptotic protein in malignant and premalignant tissue (Figure 5c)

***mcl-1* knock out.**

In order to analyze deeper the relevance of cholesterol-induced Mcl-1, a CRISPR/Cas9 system was developed, to evaluated the Mcl-1 role in cholesterol overload context, our results show that Mcl-1 is an important protein for the development of cancer, there are several reports where postulate Mcl-1 as a possible therapeutic target, given the nature

of this protein, it is involved in cell proliferation (Harley, Allan, Sanderson, & Clarke, 2010), energy metabolism, and mitochondrial dynamics (Perciavalle et al., 2012). Mcl-1 is one of the most highly amplified genes in a variety of HCC (Sieghart et al., 2006) . As a result, most therapeutic strategies have been directed at antagonizing Mcl-1 antiapoptotic activity attempting to foster malignant cell death (Yu et al., 2016).

Then a knockout was performed to evaluate the Mcl-1function when this protein is activated for the cholesterol overload.

Construction and evaluation of the CRISPR/Cas9 system.

Versatile method for genome engineering in eukaryotic cells may be a powerful and specific tool for elimination of proteins. The Cas9 endonuclease induces double-stranded breaks (DSBs) at specific DNA sequences. This sequence specificity is due to a gRNA that directs Cas9 to a 20-nt complementary sequence adjacent to a 3-nt motif (protospacer adjacent motif [PAM]) (Figure 6a).

Design of the guide RNA.

To design the gRNA sequences of the Mcl-1 gene were taken (exon 1 5,831-6,045 and exon 2 8,379-8,469). (table 1) Once the sequences were obtained, the Broad Institute software (available at http://www.broadinstitute.org/rnai/public/analysis-tools/sgrna-design) was used, which provided the best candidate gRNA sequences for the planned objectives. (Figure 6b)

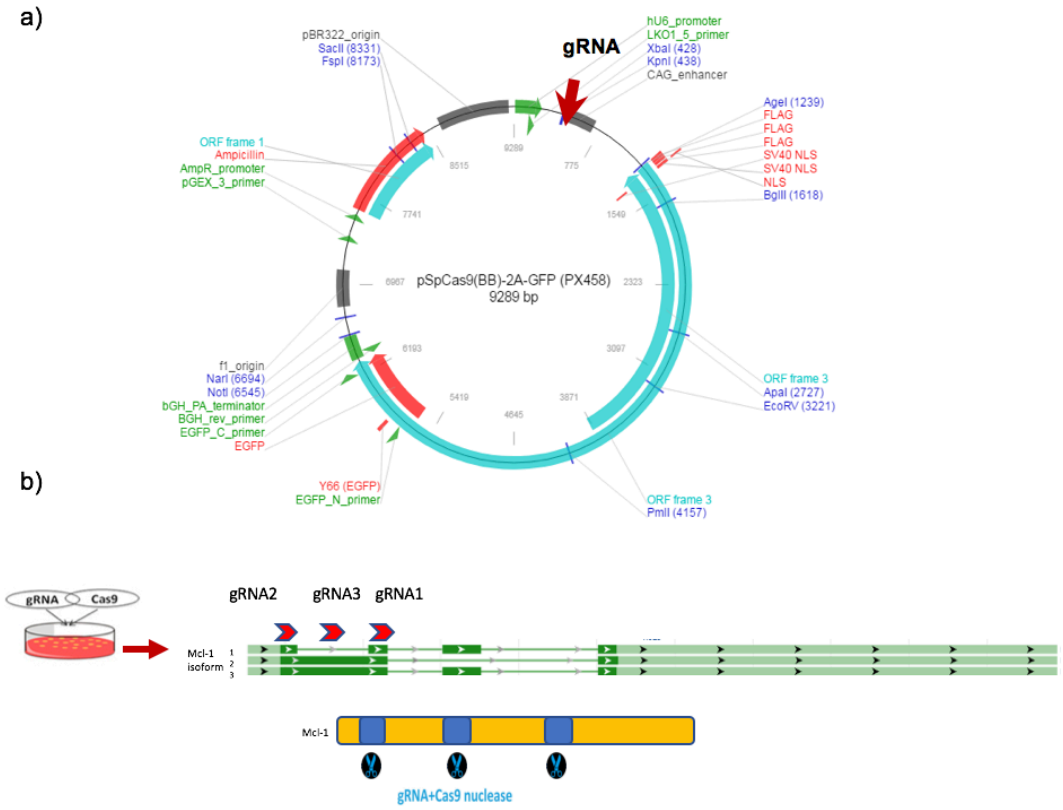

Figure 6. PX458 plasmid structure. **a)** PspCas9(BB)-2A-GFP (PX458) has 9289bp, this plasmid has a resistance gen Ampicillin, to corroborate the transfection we have a reporter gen in this case is GFP, it is just to validate the transfection efficiency. **b)** Design of the guide RNA. Three different gRNA were designed due to Mcl-1 has 3 isoforms, so it was selected the best gRNA to knockout the Mcl-1 large isoform which is the antiapoptotic one, we did an analysis in Broad Institute date base, to have the top list for gRNA.

Once the list of the gRNAs was obtained, it was verified which of them were in conserved regions of the protein. To corroborate the data obtained, the software MEGA version 6 was used to verify how conserved they were. Likewise, those candidates which their position could induce a change in the reading frame closest to the 5 ' end were selected See in table 2

Name	Orientation	sgRNA Sequence	PAM	sgRNA Context Sequence	Score
gRNA 1	sense	AGGCGCTGGAGACCTTA^CGA	CGG	AGGAAGGCGCTGGAGACCTTA^CGACGGGTT	0.7157
gRNA 2	antisense	CCAAAAGTCGCCCTCCC^GGG	CGG	GTAGCCAAAAGTCGCCCTCCC^GGGCGGGTG	0.5939
gRNA3	antisense	GAAGAAAAGCAGCCTCG^CGG	GGG	GCGCGAAGAAAAGCAGCCTCG^CGGGGGTCG	0.677

Table 2. CRISPR gRNAs targeting Mcl-1 gene designed and tested in this study. Sequences of gRNAs with the PAM region highlighted in red and the Cas9 cleavage site 3-nt upstream of PAM denoted by a red line. CRISPR specificity scores were calculated by algorithms available in http://crispr.mit.edu and the conservation of each sequence was performed across 97. Conservation percentages and nucleotide variabilities as measured by Shannon entropy.

For the gRNA design, an *in silico* analysis of the MCL-1 sequence will be performed to find sequences conserved with the PAM sequence (NGG), which serve as target for Cas9. The gRNA was cloned into the plasmid pCMV-Cas9-GFP (Figure 8b).

To determine the role of Mcl-1 in the cholesterol overload, a silencing of the gene was carried out using CRSPR/cas9. For this, it was confirmed that the gRNAs directed to this gene were incorporated in plasmid.

Analysis of the plasmid PX458 of the circular form. First an analysis was carried out by enzymatic digestion to verify the size of the plasmid and the presence of the desired fragment. All constructs were digested with KpnI and the size of the plasmid was verified as well as the expected fragments (Figure 7).

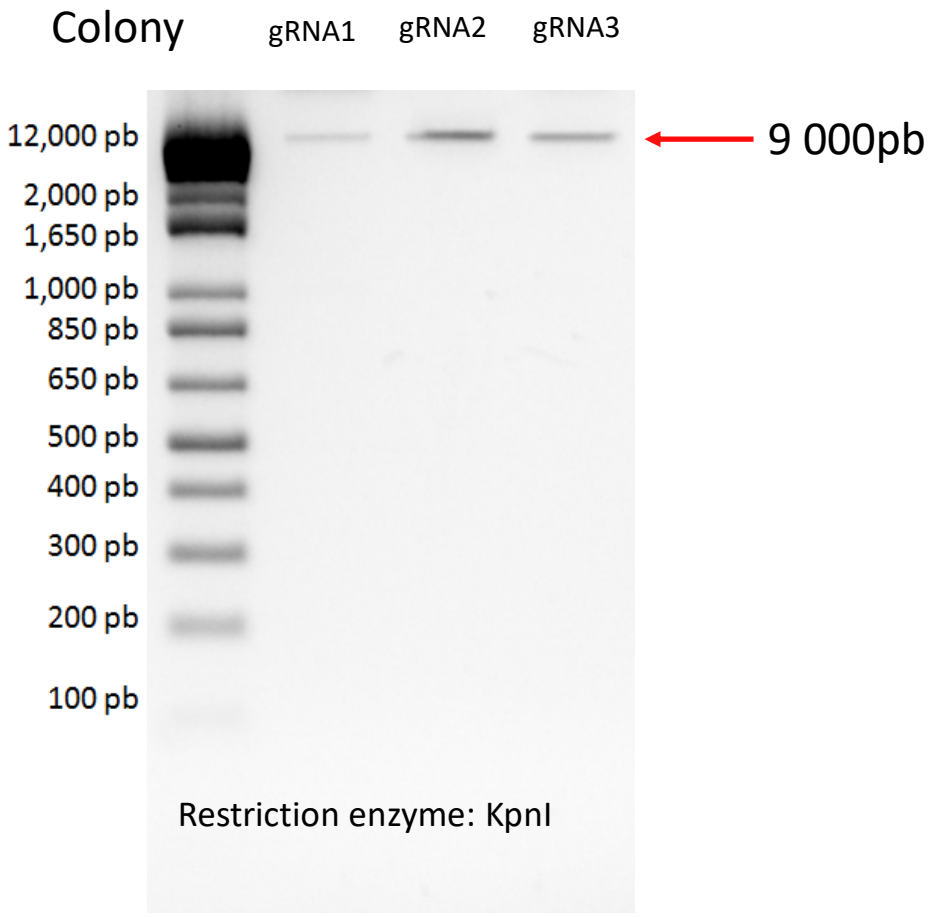

Figure 7. Restriction enzyme of PX458 plasmid 2% agarose gel showing the digestions of the plasmids corresponding to 5 colonies obtained by transforming E. coli DH5-a bacteria (lanes 1-3). The sizes obtained correspond to the expected of 9 000 bp

A PCR was performed to amplify particular regions present in each construction. For gRNA, the entire inserted fragment was amplified, as well as the fractions released

from 270 and 145 bp, the expect fraction for each of the gRNAs. These data suggest the incorporation of the gRNAs in plasmid PX458 was successfully (Figure 8).

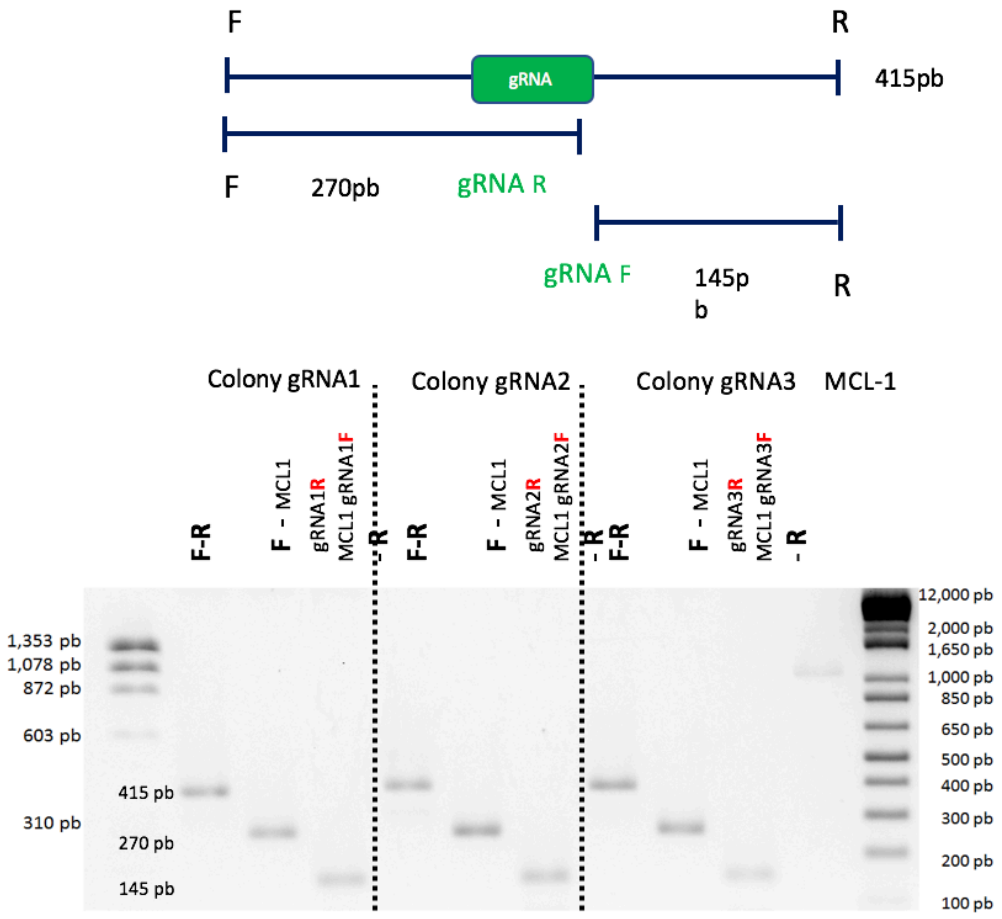

Figure 8. Amplification of the gRNAs in PX458 plasmid. PCR amplification of the ligated fragments in plasmid PX458. corresponding to the circular shapes and amplifications of the regions that include the joining regions designed for construction. Lane 1, 4 and 7, the 415 bp size band corresponding to the ligated fragment gRNA1, gRNA2, gRNA3 is observed. Amplification of the circular form of gRNA1, gRNA2, gRNA3 (lane 2, 5 and 8) of 270 bp. Amplification of the binding region gRNA1, gRNA2, gRNA3 (lane 3, 6 and 9 size of 145 bp).

The incorporation of the gRNA to the plasmid was verified by sequencing, where we can find the 3-different gRNAs were inside the PX458 plasmid,

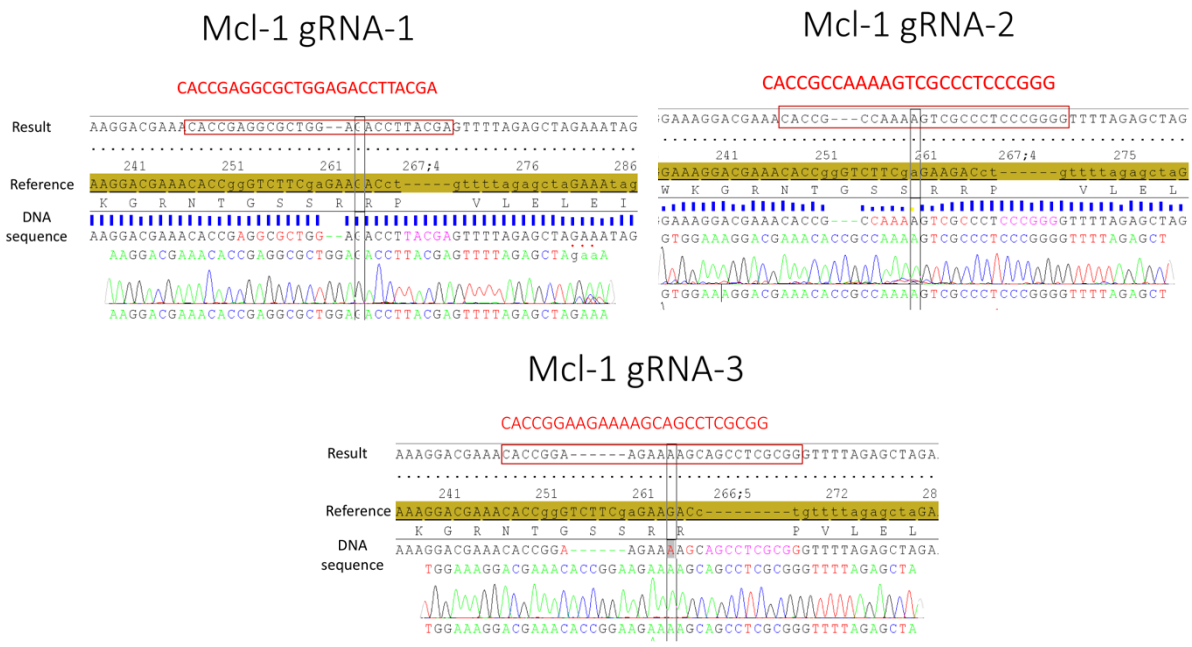

Figure 9. Sequencing of px458 plasmid. All plasmids were sequenced for each different gRNA. In every case we can found the correct sequence of the gRNA in the different plasmids.

To corroborate the ligation of the gRNAs in plasmid PX458, sequencing of plasmid PX458 and ligated gRNAs was performed (Figure 9).

After the sequencing the plasmid was ready for cell transfection now to determine the knockout of Mcl-1, a Western blot was performed against Mcl-1, where we can observe that the protein content is significantly lower compared to its control. Its means the

knockout of Mcl-1 with CRSPER/cas9 was done. We use Hek-293 because is a permissive cell line to be transfect, also we try to combinated gRNA to have a knockout, what we can found its, is necessary to use the three gRNAs. (Figure 10a)

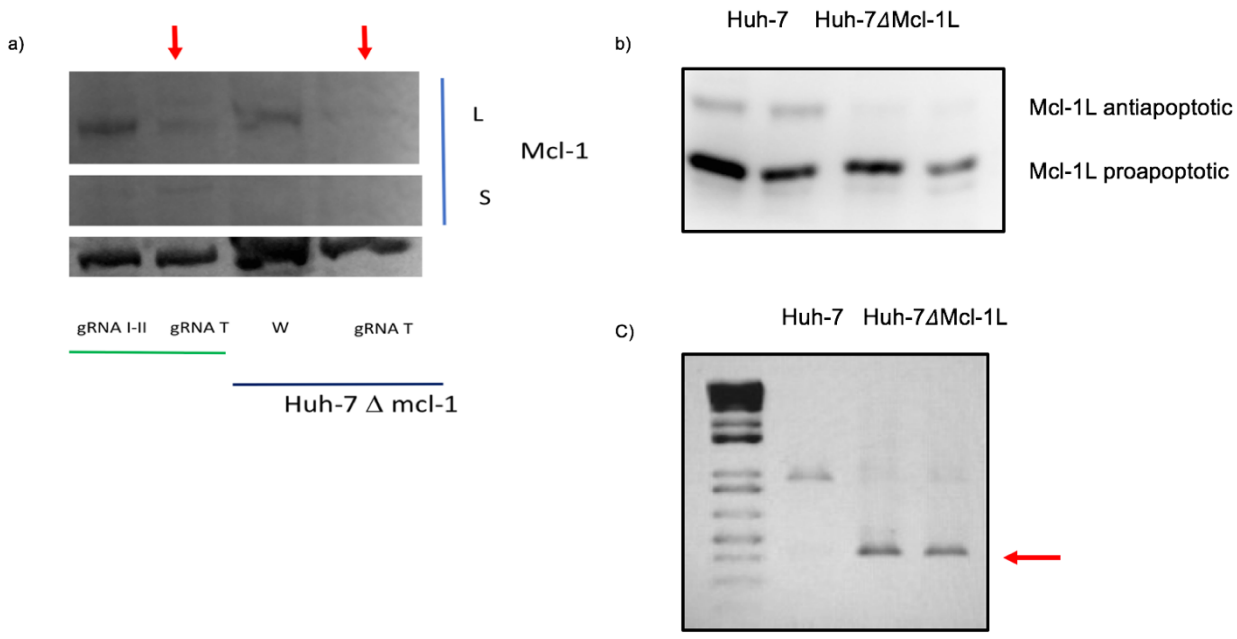

Figure 10. Knockout Mcl-1. a) Western blot was performed to evaluate the protein content of Mcl-1, lane 1 and 2 cell line Hek-293 as a transfection control, lanes 3 and 4 Huh-7 cell line. Lanes 1 and 3controls, lanes 2 and 4 Δ Mcl-1 **b)** Specific deletion of the long Mcl-1 isoform by CRISPR / Cas9. A deletion was made in the anti-apoptotic isoform of Mcl.1 a) shows protein content in Huh-7 and Huh.7 Mcl-1L cells where the presence of the longest isoform is not found, **c)** RT of Huh-7 and Huh-7 Mcl-1L where we observed a decrease in the amplification size of Mcl-1.

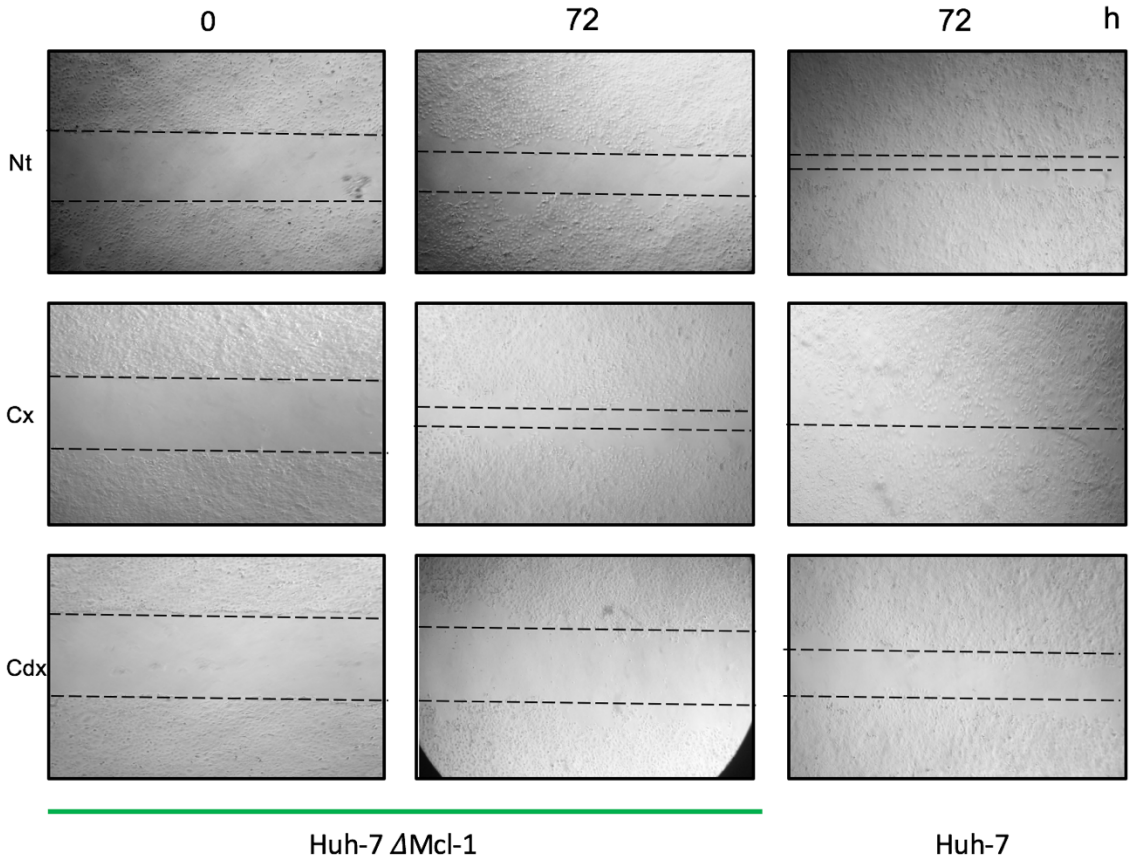

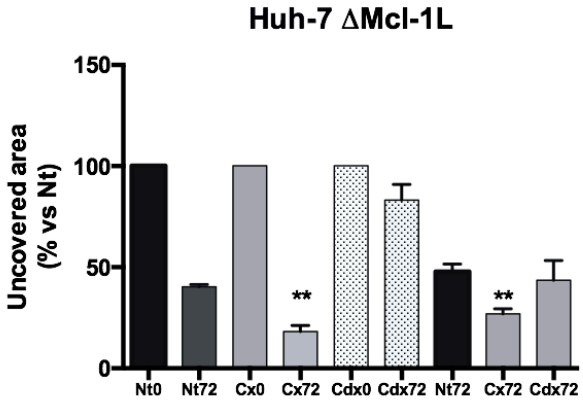

Figure 11. The presence of Mcl-1 is important for cell migration. Huh-7 and Huh-7 Mcl-1L cells were induced by Cx to undergo cell migration. Confluent monolayer of Huh-7 and Huh-7

Mcl-1Lcells were wounded with a uniform scratch, washed to remove cell debris, and cultured during 0, 4, 12, 24, 48, 72 h of incubation with Nt, Cx and Cdx. Images of cell cultures were captured at 0, 4, 12, 24, 48, 72 h after scratching, experiments were performed in the absence and presence of the selective inhibitor of DNA synthesis cytosine β-d-arabinofuranoside hydrochloride (10μM) The arrow indicates the wound edge.

Once the knockout was complete we decide to use some combination for gRNA in order to found just a specific deletion of Mcl-1L, to perform this specific deletion we only use gRNA 1 and gRNA 2 (Figure 10b), so with this specific knockout we can know if the cholesterol overload induces only the Mcl-1 large isoform, or indices all isoforms at the same time. Several studies show large isoform is one of the most implicates and overexpress in cancer (Gruber et al., 2013; V. Palve, Mallick, Ghaisas, Kannan, & Teni, 2014; V. C. Palve & Teni, 2012).

To determine the role of Mcl-1L in cellular aggressiveness, a wound healing test was performed on Huh-7 and Mcl-1LL cells. The data suggest that Mcl-1L is involved in cellular motility, since in the cell line Mcl-1L the cells migrated slower than huh-7, at 72h, huh-7 they closed the wound completely, but not the Mcl-1LL cell line even when the Cx was added the migration was not affected, the cholesterol. (Figure 11), Cholesterol overload induces cell migration even without the presence of Mcl-1L, with Cdx it was observed that both in Mcl-1LL and Huh-7 cells migration was affected.

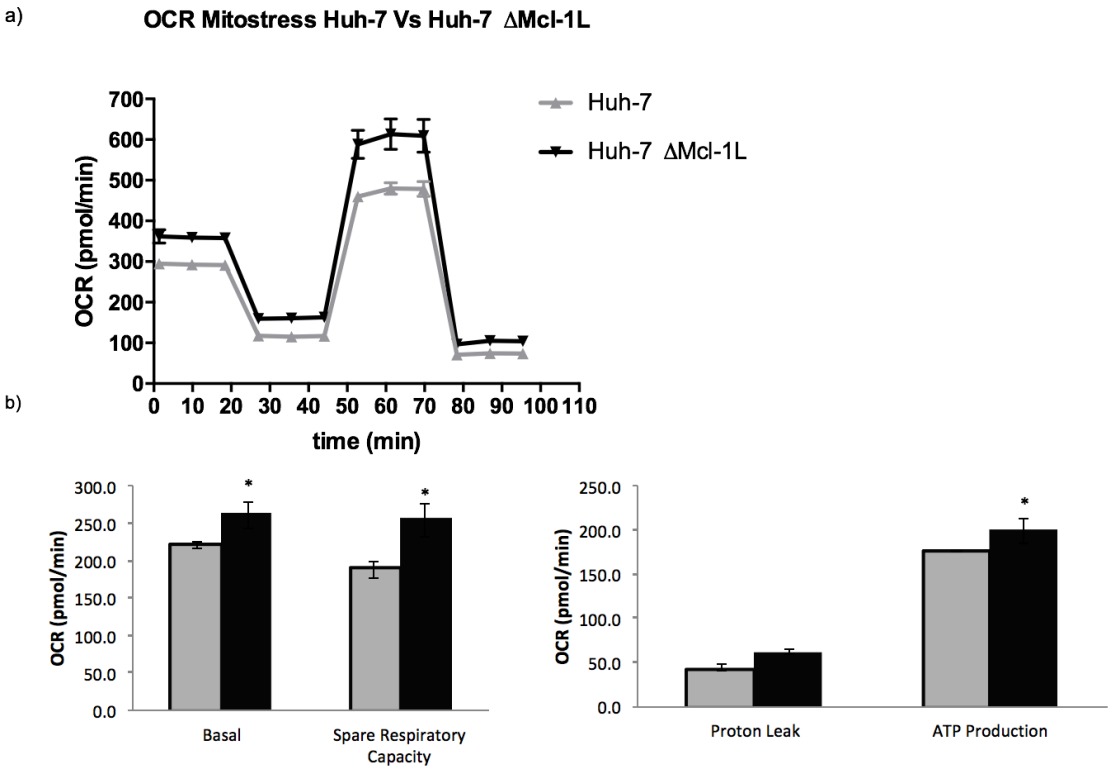

Figure 12. Huh-7 Mcl-1LL have an increased oxygen consumption rate. a) Oxygen consumption rate (OCR) was measured in control Huh-7 cells and in Huh-7 Mcl-1LL cells, with the sequential addition of different compounds: oligomycin, FCCP, Antimycin and Rotenone. **b)** different parameters of oxygen consumption as baseline, ATP production and proton leak.

The role of Mcl-1 as a metabolic modulator in hepatocarcinoma cells.

Due to Mcl-1L could be related to the regulation of cell metabolism (Thomas et al., 2010), it was decided to explore any changes in bioenergetics metabolism by using the Seahorse technology, the OCR was determined, with the use of mitostress kit. Huh-7 Mcl-1L cells had a higher mitochondrial capacity, that is, maximum respiration was

greater in Huh-7 Mcl-1L, ATP production, and basal respiration, which indicates a Clear relationship between Mcl-1L and metabolism. (Figure 12)

The result suggests that Mcl-1L could be a metabolic regulator, having more points of comparison, it's clear the Mcl-1 is necessary for the mitochondrial metabolism, making it clear that the antiapoptotic isoform is the one that is induced by the cholesterol, when we compare all the parameters like, ATP production, Proton Leak, the Huh-7 cell line whit out Mcl-1L have a better response than Huh.7

In the same way, the acidification of the extracellular medium was measured by the s Seahorse stress Glycolysis kit, to determine if the deletion of the large Mcl-1 isoform only induced mitochondrial metabolism. What we found was that the deletion of Mcl-1L also increased the acidification of the extracellular medium, so that the glycolytic capacity, as well as its reserve are greater. These data corroborate that Mcl-1L plays an important role in cellular metabolism, such that the regulation of the activity of this protein is an important point in cell transformation. (Figure13)

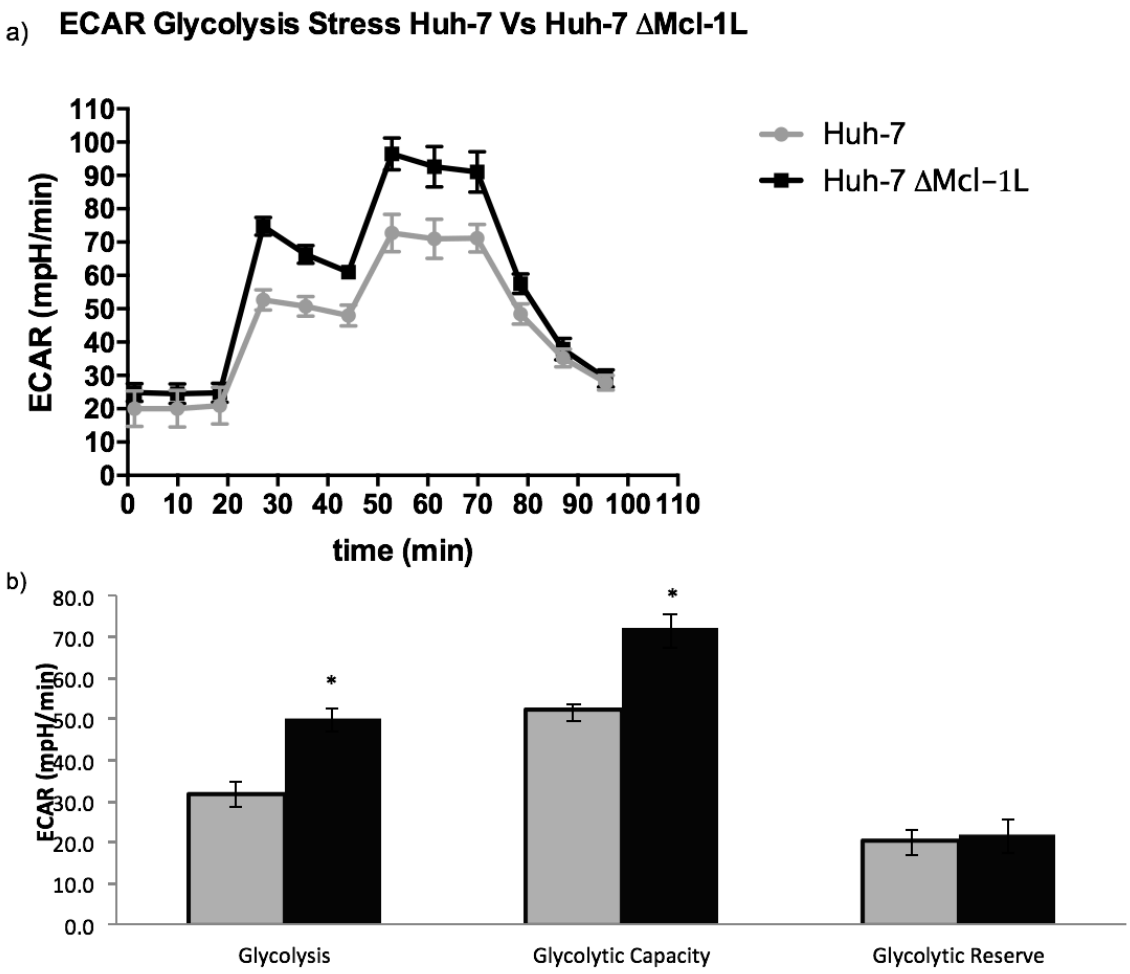

Figure 13. Huh-7 Mcl-1LL have greater acidification of the extracellular medium. a) The acidification of the medium in real time (ECAR) was measured in control Huh-7 cells and in Huh-7 Mcl-1LL cells a), with the sequential addition of different compounds: Glucose, oligomycin, 2-DG **b)** glycolytic parameters as glycolytic capacity and glycolytic reserve. form ratio (major/minor axis). Data are mean ± SEM of n = 4–6 experiments. *p < 0.05 as indicated.

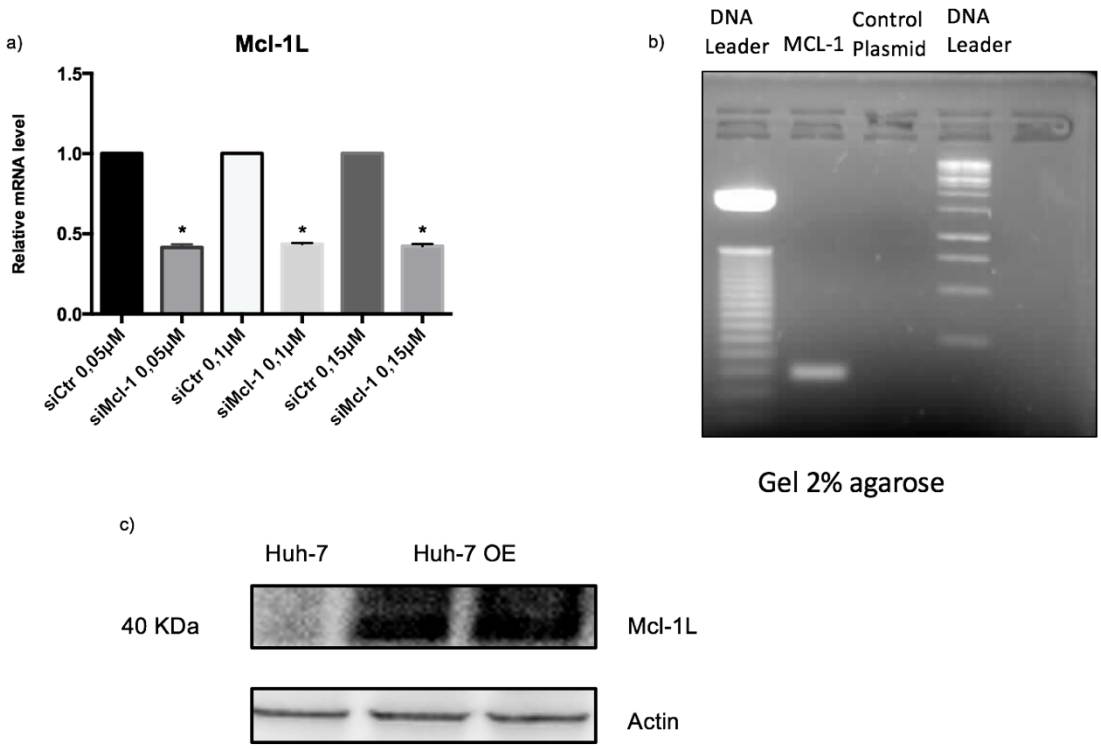

Figure 14. Silencing and overexpression of Mcl-1 a) The optimal concentration of SiMcl-1and siCtr, were determinated using Different dilutions (0.05μM, 0.1μM, 0.15μM). Each bar represents the mean S.E. of at least three different experiments. *P<0.05 vs control. **b)** Mcl-1 plasmid. 2% agarose gel showing the digestions of the plasmids corresponding to 1 colonies obtained by transforming E. coli DH5-a bacteria. The sizes obtained correspond to the expected of 5 000 bp **c)** Huh-7 cells were transfected with Mcl-1 Plasmid, a Plasmid control was used as a control, we use 1μg for each plasmid.

Global transcriptomic analysis in Huh-7 cell line

It is clear the great relevance in the cholesterol-regulated Mcl-1. To explore further, it was decided to analyze the global transcriptomic changes by Microarray. We decided to perform a different method for the downregulation of Mcl-1, in order to corroborate the results obtained with the Knockout of Mcl-1, in this way we can ensure that the data obtained in the metabolic regulation by Mcl-1, are proper of the protein and not by

random mutation related to the Cas9 system so we performed a less aggressive method where we could only decrease the presence of Mcl-1, therefore the use of RNA interference (siRNA), figure 14. Different dilutions were made (0.05μM, 0.1μM, 0.15μM) of siRNA-Mcl-1, these dilutions did not present significant differences, so in the subsequent experiments 0.05μM siRNA Mcl-1 was used. (Figure 14a)

Using the plasmid PCMV, overexpression of Mcl-1 was induced in the Huh-7 cell line, so the first step was to corroborate the presence of Mcl-1 in the construction,
for which PCR was performed against Mcl-1 and the plasmid was used without the insert as a negative control. (Figure 14b). to corroborate the overexpression of Mcl-1 a Western Blot was performed, that we found was a strong increase of Mcl-1 in compere with Huh-7 cells without transfection (Figure14c)

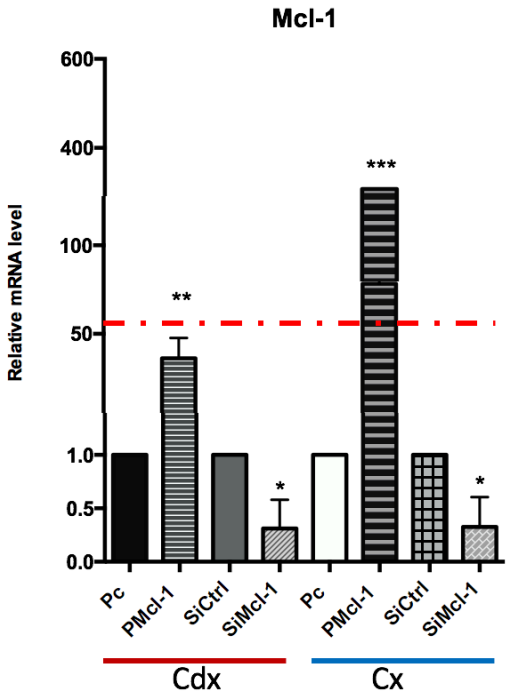

Figure 15. Mcl-1 expression with different conditions. Huh-7 cells were transfected whit Mcl-1 plasmid and Plasmid control to overexpression of Mcl-1, Mcl-1 downregulation Huh-7 were transfected whit siRNA- Mcl-1 and siCtrl and PCMV plasmid and Mcl-1 Plasmid for 72 h. after we treated with the Cx 160μg/ml and Cdx 10 mM for 90 min. Each bar represents the mean S.E. of at least three different experiments. *P<0.05; ** P<0.01; *** P<0.001 vs control Pc.

Once the optimal concentration of the different conditions to be evaluated were determined, qRT-PCR was performed evaluating the relative expression of Mcl-1 mRNA, in which we observed that the highest expression of Mcl-1 is when we treat cholesterol to Huh-7 previously transfected with plasmid PCMV-Mcl-1 having values of up to 200 times more than the control (Figure 15), this experiment was important to corroborate that all the condition works well before to do the microarray experiment, so we perform this experiment to understand what's does the cholesterol do in the cell to contribute to carcinogenesis? , and what does Mcl-1 do to help cholesterol overload? After we have all the conditions ready, now the next step was corroborating the mRNA integrity of was optima an agarose gel was made, where the 24 samples to be evaluated in the microarrays would be placed, obtaining a good mRNA integrity (Figure 16), before to do microarray experiment its necessary to have a good mRNA integrity otherwise microarray experiment cannot be done.

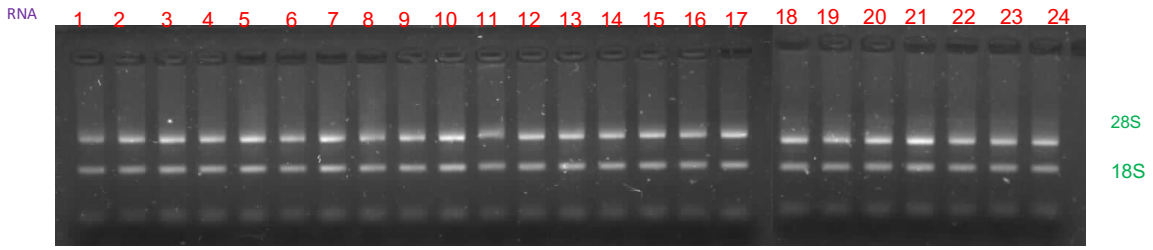

Figure 16. RNA integrity Total RNA of each condition was extracted after transfected whit Mcl-1 plasmid and Plasmid control to overexpression of Mcl-1, Mcl-1. downregulation Huh-7 were transfected whit siRNA- Mcl-1; siCtr and PCMV plasmid and Mcl-1 Plasmid for 72 h. after we treated with the Cx 160μg/ml and Cdx 15 mM for 90 min. every condition was replicate at least three different experiments.

In order to understand globally how the cholesterol overload affects the Huh-7 cell line, a transcriptomic study was carried out, in which we could determine the genes affected by cholesterol overload. The transcriptomic profile between cells with cholesterol overload and untreated was 318 differentially expressed genes. These genes were highly efficient in separating the two genotypes in an unsupervised cluster analysis These genes are upregulated (RAB27B, ACSL3, BMF, ATP2B4, TPTE2P6, TPTE2, CYP2R, STARD9) and these are some genes that are downregulated (SREBF1, MVD, TP53INP1, HMGCR, CDKN1C, IGFBP1, CDKN1A). We found that a significant number of genes were downregulated related to cholesterol biosynthesis, which is consistent with our cholesterol overload model. Interestingly we also observed that some genes related to cell cycle inhibition were downregulated, on the other hand, in gene list upregulated genes were found related to transport of fatty acids. (Figure 17)

Finally, an enrichment analysis was carried out showing that sterol biosynthesis It was diminished, that is, the plot shows a negative correlation, this confirms some genes found in the top 10 of the list of downregulated genes, on the other hand, through the use of the Kyoto Encyclopedia of Genes and Genomes, obtained (Figure 17c) the major associated signaling pathways were related to mitochondria dysfunction, fatty acid, xenobiotics and GSH metabolism, bile acids biosynthesis, oxidative phosphorylation, oxidative stress response. Consistently, affected toxicological functions were involved in liver cholestasis, steatosis, inflammation, necrosis, and cell death. Thus, the altered oxidative stress response in cholesterol overload might be responsible for the aggravated cell malignancy.

Its means that cholesterol overload, has a general impact into the cell, for one hand overexpression of Mcl-1, who induces metabolic changes, which contribute to cell transformation, and for other hand helps the inhibition of cell cycle regulators, which promote an accelerated proliferation, characteristics of cancer cells.

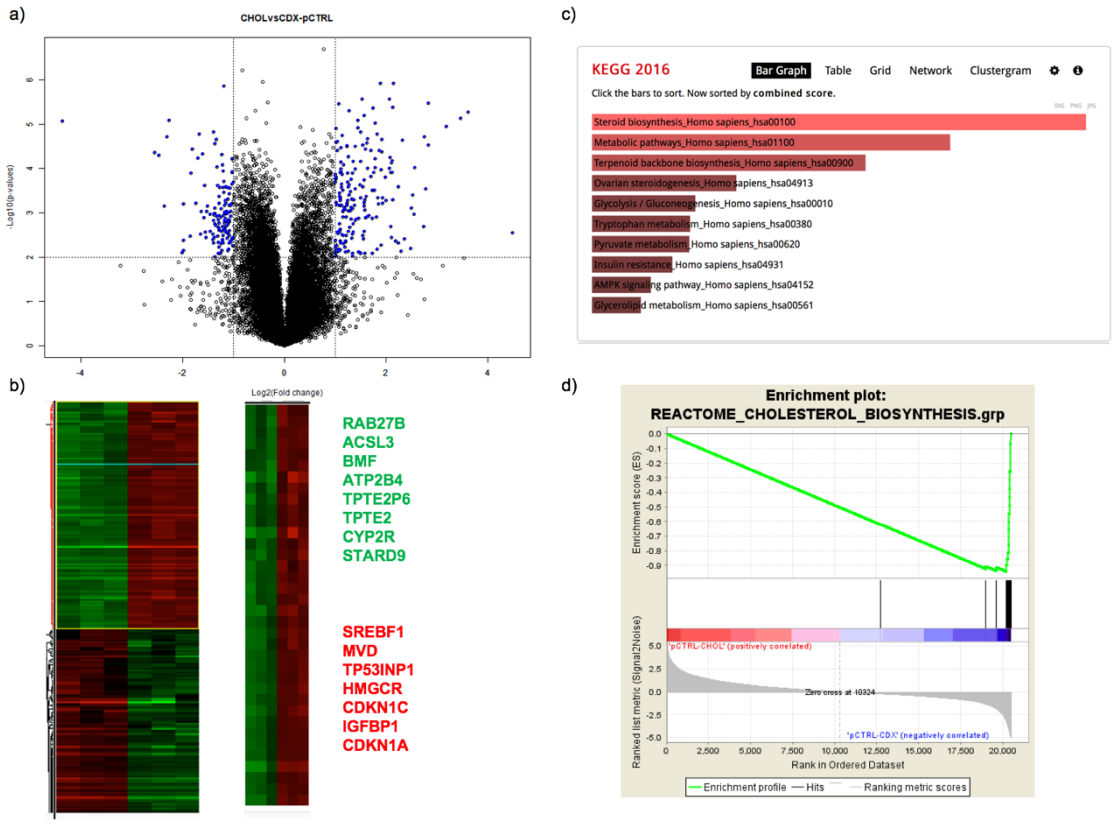

Figure 17. Global transcriptomic analysis in Huh-7 cell line. **a)** cholesterol specific gene expression signature in hepatocarcinoma cell line transfected whit Mcl-1 plasmid and Plasmid control to overexpression of Mcl-1, Mcl-1 downregulation Huh-7 were transfected whit siRNA-Mcl-1; siCtrl and PCMV plasmid and Mcl-1 Plasmid for 72 h. after we treated with the Cx 160μg/ml and Cdx 15 mM for 90 min. a) Volcano plot horizontal dashed lines, P<0.001; vertical dashed lines, fold change >2. **b)** hierarchical clustering of genes differentially expressed by Cho. **c)** Enrichment analysis of cholesterol gene signature. We use the Kyoto Encyclopedia of Genes and Genomes to generate a global reaction of cholesterol signature. Enrichment analysis of cholesterol of genes associated with steroid biosynthesis, Metabolic pathways, **d)** Gene set enrichment analysis (GSEA) of cholesterol. GSEA highlighting a Cholesterol signature enriched in the gene expression profile of Huh-7, GSEA using parameters recommended for expression datasets that contain a sample with less than 7 replicates: dataset and gene sets were converted into gene symbols, redundant probe sets were collapsed using probe medians.

Discussion.

NAFLD is the most common cause of liver disease worldwide, with a prevalence of 15%–30% in Western populations (Calzadilla and Adams, 2016), meanwhile in childhood the estimated prevalence of NAFLD in obese children is rising to 40–70%. The hallmark of NAFLD is lipid accumulation in the hepatocytes that defines liver abnormalities ranging from simple steatosis to NASH with or without cirrhosis development (Streba et al., 2015).

Previous data in our laboratory proved that the consumption of a high cholesterol diet induces a cholesterol overload in the liver rising a complex response in hepatocytes characterized by mitochondria dysfunction and oxidative stress (Enriquez-Cortina et al., 2017). All of these processes is associated to an increment in cancer cell aggressiveness. For that reason, we developed a new in vitro strategy to mimic the effects observed in mice. (Figure1) Thus, we use different cell lines to incorporate a cholesterol overload and proved that our model works in different cell lines like Huh-7, HepG2, Hep3B, and primary mouse hepatocytes. Now it's clear that the incorporation of cholesterol is completely different in each cell line, it could be associated with the capacity to manage the cholesterol, Huh-7 cells increase between 3 y 4 change when cells were treat whit Cx 160μg/ml, but HepG2 cells increase 10 times more than Huh-7, in the same way primary cell culture was 6-fold compared with control. Its mean that all the experiments were carried out with the same concentration but the cells take different amount cholesterol, if we want to compare all the cell lines effects of cholesterol overload, first is necessary to determine the optimal concentration of Cx, like in Huh-7 cell line.

Different cellular organelles have distinct and tightly regulated cholesterol content and lipid composition, with vast majority 60–90% of total cholesterol residing in the plasma membrane, the endoplasmic reticulum and mitochondria have lower content (3–5% of the total cellular cholesterol) and are highly sensitive to membrane fluidity loss induced by cholesterol enrichment (Luo et al., 2017). In figure 2 there are representative picture from Huh-7 and Hep3B cell line to address the cholesterol content when cells were treated whit Cx, after that mitochondrial was stained to know if the cholesterol overload localize into the mitochondrial.

cholesterol overload in the liver has been strongly associated to an increment of the damage due to a second insult such alcohol, bile duct ligation, or chemicals, these finding have positioned this lipid as a key determinant in the liver disease progression (Musso et al., 2013). Previous studies from our lab reported that cholesterol overload is a determinant factor that could maintain or aggravate the alcohol-induced liver damage (Lopez-Islas et al., 2016).

In the same line a wound healing experiment was perform, this time to know if the cholesterol overload increase the cell motility, based on figure 3, Huh-7 cell with cholesterol overload has a better response, for other hand when cells were treat only whit Cdx (lees cholesterol), the cells do not respond to healing.

Cdx are a family of compounds made up of sugar molecules bound together in a ring (cyclic oligosaccharides). In the food industry, Cdx are employed for the preparation of cholesterol free products: the bulky and hydrophobic cholesterol molecule is easily

lodged inside Cdx rings that are then removed.(de Oliveira et al., 2011; Marcolino, Zanin, Durrant, Benassi Mde, & Matioli, 2011).

We use Cdx as vehicle, but in our experiments, we use Cdx to determine the cell response in cholesterol absence, in the figure 4 Cdx doesn't have any effect in ROS production, but Cx have a strong increase of ROS. ROS are the main inducers of DNA damage and, consequently, of mutations. Indeed, particularly mitochondria-derived ROS have been implicated to initiation, progression and aggressiveness of cancer (Ishikawa et al., 2008). Figure 4 shows the increment of superoxide anion when cells were treated whit Cx.

In line with this experiment the induction of Mcl-1 is only present in Cx treatment and not in Cdx our data show that there are no changes in the Bcl-2 protein, however, Mcl-1 shows in increase in protein content when there is cholesterol overload, (Figure 5), this suggests that the increase of this Protein allows the inhibition of cell death. Considering Mcl-1 of great relevance, because a removal of this anti-apoptotic protein induces liver damage, fibrosis and increases the susceptibility to apoptosis in hepatocytes (Vick et al., 2009).

A high expression of Bax has been consistently associated with the decrease in the activity of Bcl-2, a pro-apoptotic protein, since the quotient between the content of these two proteins is continuously calculated to estimate the cell survival ratio (Strasser, 2005). However, the role of other members of the Bcl-2 family such as Mcl-1, which share the highest homology with Bcl-2, has been left aside.

It is well known that the expression of Mcl-1 is induced by the activation of the transcription factor STAT3. This transcription factor develops an adaptive response to aggression to the liver by amplifying genes that maintain cellular homeostasis (Szczepanek et al., 2012). Figure 5 shows that cholesterol overload induces STAT3 activation in Ser727 at 90 min, in inactive in the cytosol, but once activated by cytokines or growth factors it is phosphorylated at Tyr 705. Canonically, this phosphorylation triggers dimerization and translocation to the nucleus. Once at the nucleus, the dimer of Stat3, is phosphorylated by the kinases such as Erk1/2 in Ser 727 allowing the DNA binding and the expression of its target genes (Timofeeva et al., 2012, You et. al., 2015).

We also observed that cholesterol overload induces the expression of STAT3, where we can observe its maximum increase at 90 min. The data suggest that cholesterol overload exerts effects on STAT3 for proteins target such as Mcl-1 to function as protective proteins thus limiting apoptosis, it is important to note that this effect was not found in proteins such as Bcl-2 or even BclxL. We corroborated the expression of Mcl-1 induced by cholesterol overload by qRT-PCR.

To verify this, mice were fed a high cholesterol diet (1% cholesterol) for 8 months and received a single dose of DEN (10μg/g) as carcinogen, and the protein content of Mcl-1 was determined in tumors (T) and surrounding tissue (ST). we found that only de mice were HC diet has an increase of Mcl-1 in T and ST, but not in the mice were chow diet Mcl-1 was not present in T and ST. so these data corroborate that cholesterol overload has an impact in Mcl-1, this effect are associate whit increase of STAT3.

Gene-deletion studies have demonstrated that Mcl-1 expression is critical to the survival of multiple cellular lineages, despite the concomitant expression of other pro-survival BCL-2 proteins,(Opferman et al., 2005). However, the physiological reason why Mcl-1 is essential for promoting the survival of so many different cell types (Perciavalle et al., 2012) remains elusive. In this study, we reveal a role for Mcl-1 in induction of cholesterol overload.(Rinkenberger, Horning, Klocke, Roth, & Korsmeyer, 2000)

To understand the function of Mcl-1 in context of cholesterol overload a cell line knockout for Mcl-1 was done, by CRISPR/cas9 technology, we designed three gRNAs (Table 1) all the them were targeted to conserved sequence of Mcl-1. (Figure 6-9)

PX458 This plasmid contains two expression cassettes, hSpCas9 and the chimeric guide RNA. The vector can be digested using BbsI, and a pair of annealed oligos (design is indicated below) can be cloned into the guide RNA. The oligos is designed based on the target site sequence (20bp) and needs to be flanked on the 3' end by a 3bp NGG PAM sequence. (Figure 6)

Although the targeting specificity of Cas9 is believed to be tightly controlled by the 20-nt guide sequence of the sgRNA and the presence of a PAM adjacent to the target sequence in the genome, potential off-target cleavage activity could still occur on DNA sequence with even three to five base pair mismatches in the PAM-distal part of the

sgRNA-guiding sequence. Moreover, previous studies have demonstrated that different guide RNA structures can affect the cleavage of on-target and off-target sites. Crystal structure studies and single-molecule DNA curtain experiments suggest that while the PAM site is essential for the initiation of Cas9 binding, the seed sequence corresponding to 3′ end of the crRNA complementary recognition sequence, directly adjacent to PAM, is also critical for subsequent Cas9 binding, R-loop formation, and activation of nuclease activities in Cas9 (Zhang, Tee, Wang, Huang, & Yang, 2015).

Off-target mutations of CRISPR/Cas9 have been analyzed in previous studies of nonhuman primates, but no report has investigated genome-wide off-target effects in living monkeys. Here, we used rhesus monkeys in which a genetic disorder mimicking Duchenne muscular dystrophy had previously been produced with CRISPR/Cas9. Using whole genome sequencing to comprehensively assess on- and off-target mutations in these animals, we found that CRISPR/Cas9-based gene editing is active on the expected genomic sites without producing off-target modifications in other functional regions of the genome (Wang et al., 2018).

CRISPR/Cas9 it’s a great tool to genetic design, but this time we decided uses a knock down to study of Mcl-1, effect in order to corroborate the results in Mcl-1L by CRISPR/Cas9, if the data show us the same effect in bout condition (knock out and knock down). We can say that the effect of the deletion of Mcl-1 is proper to the protein function and not by an Off-target mutation.

Mcl-1 is a unique anti-apoptotic Bcl-2 family member that its genetic ablation results in cell autonomous deficiencies in a myriad of cellular lineages (Beroukhim et al., 2010).

However, Mcl-1 gene ablation disables both its anti-apoptotic activity at the OMM as well as its ability to facilitate mitochondrial function within the matrix. For this reason, it will be important to determine the relative contributions of Mcl-1's different functional roles for promoting the survival and development of hematopoietic and other cell lineages. Mcl-1's critical function during these stages may merely be to support cell survival by antagonizing apoptosis. However, Mcl-1 may also facilitate mitochondrial fitness during cellular proliferation and differentiation when metabolic demands on the mitochondria are modulated.

Mcl-1 is one of the most highly amplified genes in many human cancers (Beroukhim et al., 2010). As a result, most therapeutic strategies have been directed at antagonizing Mcl-1 anti-apoptotic activity attempting to foster malignant cell death. However, these findings raise the possibility that the non-apoptotic function of Mcl-1 may also fuel mitochondrial function in cancer cells, thus facilitating the generation of mitochondria-derived substrates required to maintain the levels of biomolecular synthesis that drives hyper-proliferation (Deberardinis, Sayed, Ditsworth, & Thompson, 2008). Therefore, inhibiting Mcl-1 ability to promote mitochondrial function may represent a new therapeutic target in cancer cells. (Figure 12-13).

Microarray data were first normalized by using the quantile normalization algorithm. As shown, this normalization method corrected putative technical variations between samples. Without initial gene filtration, Principal Component Analysis (PCA) using expression values of all genes in all 24 samples mostly separated cholesterol from non-

cholesterol samples. (Figure 17) Then, a filtration by “flag” and “signal intensity” was applied. Were retained only the entities in which at least 50% of the values in any of the two conditions. For the filtration by signal intensity, were retained the entities in which at least 50% of the values in any of the two conditions were within the range of interest. Differentially expressed genes were identified by a two-sample univariate t-test and a random variance model. As previous report (Sulpice et al., 2016)

One of our main interest was to address the gene expression profile induced by cholesterol overload, induced dysregulation 318 genes, indicating a prominent impact in gene expression tending to an adaptive response, that could be related, among other physiological processes, to apoptosis resistance in a mechanism involving mitochondria homeostasis and function, narrowed linked to changes in mitochondria redox state. Consistent with our previous data in change of metabolic parameter, microarray data show that metabolism pathways had strong impact derived by cholesterol overload, through overexpression of Mcl-1who is the modulator of metabolism according to data obtained.

Consistent with our previous findings in a mice model of HCC (Enríquez-Cortina et al., 2017), previous work we have reported that under HC diet, and in the presence of a carcinogenic stimulus, mice develop an aggressive phenotype of HCC (Enríquez-Cortina et al., 2017), correlating with the present transcriptomic data; interestingly, cholesterol overload has a high impact in some process like, proliferation, migration,

metabolic pathway, redox state. (Dominguez-Perez et al., 2016; Enriquez-Cortina et al., 2017; Nuno-Lambarri et al., 2016).

Conclusion.

In summary, the cholesterol overload induced the expression of Mcl-1, this over-expression seems to be specific to the antiapoptotic isoform, in addition this isoform has a close relationship in metabolic pathways. These data strongly support the premise that cholesterol overload accelerates the process of carcinogenesis, and one of the ways is to overexpress antiapoptotic proteins such as Mcl-1, which besides protecting the cell against apoptosis, also contribute to the development of cellular transformation through the modulation of metabolic pathways.

Reference.

Aceves-Martins, M., Llaurado, E., Tarro, L., et al. (2016). Obesity-promoting factors in Mexican children and adolescents: challenges and opportunities. *Glob Health Action, 9*, 29625.

Baulies, A., Montero, J., Matias, N., et al. (2018). The 2-oxoglutarate carrier promotes liver cancer by sustaining mitochondrial GSH despite cholesterol loading. *Redox Biol, 14*, 164-177.

Bellentani, S. (2017). The epidemiology of non-alcoholic fatty liver disease. *Liver Int, 37 Suppl 1*, 81-84.

Beroukhim, R., Mermel, C. H., Porter, D., et al. (2010). The landscape of somatic copy-number alteration across human cancers. *Nature, 463*(7283), 899-905.

Chen, H., & Chan, D. C. (2005). Emerging functions of mammalian mitochondrial fusion and fission. *Hum Mol Genet, 14 Spec No. 2*, R283-289.

Coulouarn, C., Corlu, A., Glaise, D., et al. (2012). Hepatocyte-stellate cell cross-talk in the liver engenders a permissive inflammatory microenvironment that drives progression in hepatocellular carcinoma. *Cancer Res, 72*(10), 2533-2542.

Cronin, K. A., Lake, A. J., Scott, S., et al. (2018). Annual Report to the Nation on the Status of Cancer, part I: National cancer statistics. *Cancer, 124*(13), 2785-2800.

Dang, C. V. (2012). Links between metabolism and cancer. *Genes Dev, 26*(9), 877-890.

Day, C. L., Chen, L., Richardson, S. J., et al. (2005). Solution structure of prosurvival Mcl-1 and characterization of its binding by proapoptotic BH3-only ligands. *J Biol Chem, 280*(6), 4738-4744.

de Oliveira, V. E., Almeida, E. W., Castro, H. V., et al. (2011). Carotenoids and beta-cyclodextrin inclusion complexes: Raman spectroscopy and theoretical investigation. *J Phys Chem A, 115*(30), 8511-8519.

Deberardinis, R. J., Sayed, N., Ditsworth, D., et al. (2008). Brick by brick: metabolism and tumor cell growth. *Curr Opin Genet Dev, 18*(1), 54-61.

Dominguez-Perez, M., Nuno-Lambarri, N., Clavijo-Cornejo, D., et al. (2016). Hepatocyte Growth Factor Reduces Free Cholesterol-Mediated Lipotoxicity in Primary Hepatocytes by Countering Oxidative Stress. *Oxid Med Cell Longev, 2016*, 7960386.

Dutta, R., & Mahato, R. I. (2017). Recent advances in hepatocellular carcinoma therapy. *Pharmacol Ther*.

Elgendy, M., Abdel-Aziz, A. K., Renne, S. L., et al. (2017). Dual modulation of MCL-1 and mTOR determines the response to sunitinib. *J Clin Invest, 127*(1), 153-168.

Elgendy, M., & Minucci, S. (2015). A novel autophagy-independent, oncosuppressive function of BECN1: Degradation of MCL1. *Autophagy, 11*(3), 581-582.

Enriquez-Cortina, C., Almonte-Becerril, M., Clavijo-Cornejo, D., et al. (2013). Hepatocyte growth factor protects against isoniazid/rifampicin-induced oxidative liver damage. *Toxicol Sci, 135*(1), 26-36.

Enriquez-Cortina, C., Bello-Monroy, O., Rosales-Cruz, P., et al. (2017). Cholesterol overload in the liver aggravates oxidative stress-mediated DNA damage and accelerates hepatocarcinogenesis. *Oncotarget, 8*(61), 104136-104148.

Garcia-Ruiz, C., Ribas, V., Baulies, A., et al. (2016). Mitochondrial Cholesterol and the Paradox in Cell Death. *Handb Exp Pharmacol*.

Gomez-Quiroz, L. E., Factor, V. M., Kaposi-Novak, P., et al. (2008). Hepatocyte-specific c-Met deletion disrupts redox homeostasis and sensitizes to Fas-mediated apoptosis. *J Biol Chem, 283*(21), 14581-14589.

Gomez-Quiroz, L. E., Seo, D., Lee, Y. H., et al. (2016). Loss of c-Met signaling sensitizes hepatocytes to lipotoxicity and induces cholestatic liver damage by aggravating oxidative stress. *Toxicology, 361-362*, 39-48.

Gruber, S., Straub, B. K., Ackermann, P. J., et al. (2013). Obesity promotes liver carcinogenesis via Mcl-1 stabilization independent of IL-6Ralpha signaling. *Cell Rep, 4*(4), 669-680.

Hanahan, D., & Weinberg, R. A. (2011). Hallmarks of cancer: the next generation. *Cell, 144*(5), 646-674.

Harley, M. E., Allan, L. A., Sanderson, H. S., et al. (2010). Phosphorylation of Mcl-1 by CDK1-cyclin B1 initiates its Cdc20-dependent destruction during mitotic arrest. *EMBO J, 29*(14), 2407-2420.

He, M., Zhang, W., Dong, Y., et al. (2017). Pro-inflammation NF-kappaB signaling triggers a positive feedback via enhancing cholesterol accumulation in liver cancer cells. *J Exp Clin Cancer Res, 36*(1), 15.

Hwang, S., Hartman, I. Z., Calhoun, L. N., et al. (2016). Contribution of Accelerated Degradation to Feedback Regulation of 3-Hydroxy-3-methylglutaryl Coenzyme A Reductase and Cholesterol Metabolism in the Liver. *J Biol Chem, 291*(26), 13479-13494.

Ikonen, E. (2008). Cellular cholesterol trafficking and compartmentalization. *Nat Rev Mol Cell Biol, 9*(2), 125-138.

Ishikawa, K., Takenaga, K., Akimoto, M., et al. (2008). ROS-generating mitochondrial DNA mutations can regulate tumor cell metastasis. *Science, 320*(5876), 661-664.

Jimenez-Salazar, J. E., Posadas-Rodriguez, P., Lazzarini-Lechuga, R. C., et al. (2014). Membrane-initiated estradiol signaling of epithelial-mesenchymal transition-associated mechanisms through regulation of tight junctions in human breast cancer cells. *Horm Cancer, 5*(3), 161-173.

Li, M. X., & Dewson, G. (2015). Mitochondria and apoptosis: emerging concepts. *F1000Prime Rep, 7*, 42.

Liu, W., Baker, R. D., Bhatia, T., et al. (2016). Pathogenesis of nonalcoholic steatohepatitis. *Cell Mol Life Sci, 73*(10), 1969-1987.

Lopez-Islas, A., Chagoya-Hazas, V., Perez-Aguilar, B., et al. (2016). Cholesterol Enhances the Toxic Effect of Ethanol and Acetaldehyde in Primary Mouse Hepatocytes. *Oxid Med Cell Longev, 2016*, 9209825.

Ludwig, J., Viggiano, T. R., McGill, D. B., et al. (1980). Nonalcoholic steatohepatitis: Mayo Clinic experiences with a hitherto unnamed disease. *Mayo Clin Proc, 55*(7), 434-438.

Maierean, S., Serban, M. C., Rizzo, M., et al. (2017). The potential role of mitochondrial ATP synthase inhibitory factor 1 (IF1) in coronary heart disease: a literature review. *Lipids Health Dis, 16*(1), 35.

Marcolino, V. A., Zanin, G. M., Durrant, L. R., et al. (2011). Interaction of curcumin and bixin with beta-cyclodextrin: complexation methods, stability, and applications in food. *J Agric Food Chem, 59*(7), 3348-3357.

Mari, M., Colell, A., Morales, A., et al. (2010). Redox control of liver function in health and disease. *Antioxid Redox Signal, 12*(11), 1295-1331.

Nuno-Lambarri, N., Dominguez-Perez, M., Baulies-Domenech, A., et al. (2016). Liver Cholesterol Overload Aggravates Obstructive Cholestasis by Inducing Oxidative Stress and Premature Death in Mice. *Oxid Med Cell Longev, 2016*, 9895176.

Opferman, J. T., Iwasaki, H., Ong, C. C., et al. (2005). Obligate role of anti-apoptotic MCL-1 in the survival of hematopoietic stem cells. *Science, 307*(5712), 1101-1104.

Ophinni, Y., Inoue, M., Kotaki, T., et al. (2018). CRISPR/Cas9 system targeting regulatory genes of HIV-1 inhibits viral replication in infected T-cell cultures. *Sci Rep, 8*(1), 7784.

Palve, V., Mallick, S., Ghaisas, G., et al. (2014). Overexpression of Mcl-1L splice variant is associated with poor prognosis and chemoresistance in oral cancers. *PLoS One, 9*(11), e111927.

Palve, V. C., & Teni, T. R. (2012). Association of anti-apoptotic Mcl-1L isoform expression with radioresistance of oral squamous carcinoma cells. *Radiat Oncol, 7*, 135.

Perciavalle, R. M., Stewart, D. P., Koss, B., et al. (2012). Anti-apoptotic MCL-1 localizes to the mitochondrial matrix and couples mitochondrial fusion to respiration. *Nat Cell Biol, 14*(6), 575-583.

Ribas, V., Garcia-Ruiz, C., & Fernandez-Checa, J. C. (2014). Glutathione and mitochondria. *Front Pharmacol, 5*, 151.

Ribas, V., Garcia-Ruiz, C., & Fernandez-Checa, J. C. (2016). Mitochondria, cholesterol and cancer cell metabolism. *Clin Transl Med, 5*(1), 22.

Rinkenberger, J. L., Horning, S., Klocke, B., et al. (2000). Mcl-1 deficiency results in peri-implantation embryonic lethality. *Genes Dev, 14*(1), 23-27.

Rosales-Cruz, P., Dominguez-Perez, M., Reyes-Zarate, E., et al. (2018). Cadmium exposure exacerbates hyperlipidemia in cholesterol-overloaded hepatocytes via autophagy dysregulation. *Toxicology, 398-399*, 41-51.

Ryerson, A. B., Eheman, C. R., Altekruse, S. F., et al. (2016). Annual Report to the Nation on the Status of Cancer, 1975-2012, featuring the increasing incidence of liver cancer. *Cancer*.

Schwickart, M., Huang, X., Lill, J. R., et al. (2010). Deubiquitinase USP9X stabilizes MCL1 and promotes tumour cell survival. *Nature, 463*(7277), 103-107.

Sieghart, W., Losert, D., Strommer, S., et al. (2006). Mcl-1 overexpression in hepatocellular carcinoma: a potential target for antisense therapy. *J Hepatol, 44*(1), 151-157.

Singh, S., Allen, A. M., Wang, Z., et al. (2015). Fibrosis progression in nonalcoholic fatty liver vs nonalcoholic steatohepatitis: a systematic review and meta-analysis of paired-biopsy studies. *Clin Gastroenterol Hepatol, 13*(4), 643-654 e641-649; quiz e639-640.

Sulpice, L., Desille, M., Turlin, B., et al. (2016). Gene expression profiling of the tumor microenvironment in human intrahepatic cholangiocarcinoma. *Genom Data, 7*, 229-232.

Thomas, L. W., Lam, C., & Edwards, S. W. (2010). Mcl-1; the molecular regulation of protein function. *FEBS Lett, 584*(14), 2981-2989.

Wallace, D. C. (2005). A mitochondrial paradigm of metabolic and degenerative diseases, aging, and cancer: a dawn for evolutionary medicine. *Annu Rev Genet, 39*, 359-407.

Wang, S., Ren, S., Bai, R., et al. (2018). No off-target mutations in functional genome regions of a CRISPR/Cas9-generated monkey model of muscular dystrophy. *J Biol Chem, 293*(30), 11654-11658.

Yu, Q., Liu, Z. Y., Chen, Q., et al. (2016). Mcl-1 as a potential therapeutic target for human hepatocelluar carcinoma. *J Huazhong Univ Sci Technolog Med Sci, 36*(4), 494-500.

Zafrir, B., Jubran, A., Lavie, G., et al. (2017). Clinical Features and Gaps in the Management of Probable Familial Hypercholesterolemia and Cardiovascular Disease. *Circ J*.

Zhang, X. H., Tee, L. Y., Wang, X. G., et al. (2015). Off-target Effects in CRISPR/Cas9-mediated Genome Engineering. *Mol Ther Nucleic Acids, 4*, e264.

Zhen, M. C., Wang, F. Q., Wu, S. F., et al. (2017). Identification of mTOR as a primary resistance factor of the IAP antagonist AT406 in hepatocellular carcinoma cells. *Oncotarget, 8*(6), 9466-9475.